*Final Draft*
**of the original manuscript:**

Behnert, I.; Matthias, V.; Doerffer, R.:
**Aerosol climatology from ground-based measurements for the southern North Sea**
In: Atmospheric Research (2007) Elsevier

DOI: 10.1016/j.atmosres.2006.05.006

# Aerosol climatology from ground based measurements for the southern North Sea

**Irina Behnert[a, c *], Volker Matthias[a, b *], Roland Doerffer[a]**

[a]*Institute for Coastal Research, GKSS, Max-Planck-Strasse 1, Geesthacht, 21502-D, Germany*
[b]*Max-Planck-Institut für Meteorologie, Bundesstrasse 55, Hamburg, 20146-D, Germany*
[c]*CIMEL Electronique, 172 Rue de Charonne, 75011-F, France*

## Abstract

An aerosol climatology over the southern North Sea region has been set up using aerosol optical properties derived from regular sunphotometer (AERONET) and lidar (EARLINET) measurements between April and September for the years 2000 to 2003. Data from four AERONET sites in the North Sea coastal region (Helgoland Island, Oostende, Hamburg and Lille) and, for comparison purposes, also from two "maritime sites" (Rame Head and Azores Island) are selected. The variability of the aerosol optical depth $\tau_a(500)$ and the spatial distribution of aerosol optical depth $\tau_a(500)$, Ångström wavelength exponent $\alpha_{440-870}$, as well as of retrieved microphysical aerosol parameters (single scattering albedo, index of refraction, particle size distribution) are studied. The four years of observations show great similarities between the North Sea coastal sites and Helgoland Island. Although 70 km separated from the coast, the aerosol optical properties found at the island are much closer to those at Hamburg, Oostende and Lille than at the maritime sites Rame Head and Azores.

Compared to the standard aerosol models differences in the Ångström wavelength exponent $\alpha_{440-870}$, the single scattering albedo and the refractive index are detected. Based on these observations a new aerosol model for the atmospheric correction of coastal water reflectance spectra of the imaging spectrometer MERIS/ENVISAT was set up, which meets in particular the higher Ångström wavelength exponent of the coastal sites compared to standard maritime conditions.

*Keywords:* Aerosols; Sunphotometer; Lidar; Atmospheric correction

[*]Corresponding authors. Tel.: +49-4152-872346
*E-mail addresses*: irina.behnert@gkss.de (Irina Behnert), Volker.Matthias@gkss.de (Volker Matthias)

## 1. Introduction

Monitoring of coastal waters are of increasing importance because these regions are highly populated and economically exploited. To improve and optimize the monitoring capability for these dynamic areas satellite data are of high interest. The Medium Resolution Imaging Spectrometer MERIS on ENVISAT (ESA, launch March 2002) with its 15 spectral bands, a spatial resolution of 300 m and a revisit period of 2-3 days provides the possibility to determine concentration fields of phytoplankton, suspended particles and yellow substances also in coastal waters, which are important water quality indicators. Prerequisite, however, is a precise atmospheric correction, which, in turn, requires the knowledge of the regional aerosol optical properties.

The atmospheric correction algorithm over open ocean areas is generally based on the assumption of the "black pixels" in the near infrared (NIR), where water is totally absorbing. The signal at the top of the atmosphere (TOA) is in this case the atmospheric path radiance, which is the result of scattering and absorption by aerosols and thin clouds, Rayleigh scattering by molecules and absorption by water vapour, ozone and other atmospheric trace gases and comprises also the specular reflectance of direct sun light or scattered light. This information and the spectral dependence predicted by a selected aerosol model is used to extrapolate the aerosol optical depth and the path radiance from NIR to the visible part of the spectrum (VIS) and thus to determine the water leaving radiance reflectance in VIS, from which, in turn the concentrations of water constituents are retrieved.

The standard aerosol models used as the basis in the MERIS atmospheric correction algorithm over ocean by Antoine and Morel (2000) are those described in the WCP-112 (1986) and by Shettle and Fenn (1979). The physico-chemical parameters (shape, size, refractive index) for the basic aerosol components "dust-like", "water-soluble", "oceanic", "soot" and "stratospheric particles" are given. Their external mixing (no physical or chemical interactions between particles of these components are assumed) in different percentages form the standard aerosol models "maritime", "urban/industrial", "continental", "stratospheric" and "volcanic". The aerosol particles are assumed to be spherical and the Mie theory (Mie, 1908; Bohren and Huffman, 1983; Wiscombe, 1996) is applied to calculate their optical properties as spectral extinction, scattering and absorption coefficients, single scattering albedo and the asymmetry parameter of the phase function. Vertical distributions of the radiatively active gases and of the atmospheric aerosols with different aerosol model settings between 0 and 50 km are recommended for various types of environments and seasons.

More realistic data sets for the radiative transfer simulations than the WCP-112 are reported in the Global Aerosol Data Set – GADS (Koepke et al., 1997; Hess et al., 1998). GADS is the result of the compilation of available measured data and extensive models with the software OPAC (Optical properties of aerosols and clouds). The global aerosol radiative forcing recommended by GADS on a grid of 5 degrees longitude and latitude is valid for average maritime, urban or continental conditions within summer and wintertime.

The atmospheric correction of satellite derived radiances over coastal waters is a further challenge. The effects of high suspended matter concentrations on the reflectances in the NIR bands, cirrus clouds, foam produced by algae, adjacency effects due to neighbouring land pixels, are only some of the issues. Several authors (Gordon, 1997; Kaufman et al., 1997; Antoine and Morel, 1999) focussed on the unresolved questions of the atmospheric correction of ocean colour imagery related to the aerosol radiative forcing. This is extremely critical for the regions characterised by strong anthropogenic influence with a high aerosol loading including absorbing particles. Additionally, the assumption of the "black pixel" in the NIR can not be applied for coastal turbid waters, because the water-leaving radiance is influenced by scattering on inorganic suspended particles. An atmospheric correction algorithm for MERIS (which can be adapted also for other ocean colour sensors) based on a multiple non-

linear regression method "Neural Network" – NN, is proposed by Doerffer and Schiller (1997; 2002). This algorithm takes into consideration the effect of the suspended scattering particles and multiple scattering effects by using an ocean-atmosphere Monte Carlo photon tracing model. The data set for training and testing the NN is produced by radiative transfer simulations, which actually use the aerosol optical properties recommended by Shettle and Fenn (1979) and WCP-112 (1986). In the coastal regions of northern Europe the limits of the anthropogenic influence are changing continuously connected with the meteorological situation. The standard aerosol models actually used in the atmospheric correction or the Global Aerosol Data Set (GADS, Koepke et al., 1997, Hess et al., 1998) do not cover the whole range of the aerosol types and concentrations available. Significant improvements of the atmospheric correction in the coastal regions of the North Sea are expected if realistic aerosol models would be used to derive the atmospheric path radiance to train the NN, i.e. where the regional distribution, the microphysics and the vertical distribution of the aerosols are applied to build the correction model.

The present work is focused on the improvement of the optical properties of the aerosol models used for the atmospheric correction over turbid coastal waters in the southern North Sea region. A regional aerosol climatology obtained from ground-based measurements as AERONET sunphotometers (Holben et al., 1998) and lidar for the region of interest is more precise for the purpose of the atmospheric correction (Gordon, 1997; Antoine and Morel, 1999). The use of a regional climatology, composed of time and region specific aerosol information can avoid the selection of unrealistic mixtures of aerosol components. This climatology can not be obtained from satellite remote sensing data of any sensor because the validation of the aerosol parameters (aerosol optical depth, Ångström wavelength exponent) for the coastal regions is not enough precise (Park et al., 2004; Robles Gonzalez et al., 2003).

The diurnal and annual cycle of the aerosol optical properties in the German Bight and in the neighbouring regions have been derived from sunphotometer measurements as well as the vertical extinction from lidar profiles using data from 2000-2003. Links between the aerosol optical properties and the synoptic air mass types are established using a method similar to that by Smirnov et al. (1994; 1995).

The results are compared with the aerosol parameters established on basis of AERONET data for the key aerosol types “dust”, “maritime”, “urban-industrial” and “biomass burning”, (Tanré et al., 2001; Dubovik et al., 2002; Smirnov et al., 2003).

## 2. Methods and data

### *2.1 Sunphotometry*

#### *2.1.1 Methods*

The sunphotometry technique gives information about the aerosol optical properties in the total atmospheric column for clear-sky conditions, similar to those requested by the satellite imagery. The principle and the errors related to this technique are described by different authors (Kaufman et al., 1997; Holben et al. 1998; Rollin, 2000).

The aerosol optical depth is derived from direct solar irradiance measurements in several spectral bands. The aerosol optical depth $\tau_a(\lambda)$ is the vertical integral of the aerosol extinction coefficient $\sigma_e(\lambda)$. The spectral dependence of the aerosol optical depth is represented by the Ångström wavelength exponent $\alpha$, which is correlated with the size distribution of the atmospheric particles (Junge, 1952). Small particles show a more pronounced wavelength dependence with larger optical depths at shorter wavelengths than

large particles. Large values of $\alpha$ represent smaller particles while smaller $\alpha$-values represent larger particles.

The aerosol monitoring is performed worldwide in the framework of AERONET (Aerosol Robotic Network,http://aeronet.gsfc.nasa.gov/). The calibration of instruments, the data processing, the accuracy of measured and retrieved data to get a quality assured data set are described in several publications (Holben et al. 1998; Smirnov at al. 2000; Dubovik et al. 2000; Holben at al. 2001). However, there are still some problems in the automatic detection of the fine cirrus, which sometimes causes unrealistically high $\tau_a(\lambda)$ and lower Ångström wavelength exponents. The aerosol optical depth $\tau_a(\lambda)$ at up to seven wavelengths (340, 380, 440, 500, 670, 870, 1020nm), where the total uncertainty in the $\tau_a(\lambda)$ retrieval is between 0.01 and 0.02, with higher errors in the ultraviolet spectral region (Eck et al., 1999; Holben et al., 2001).The columnar water vapour content is determined at 940nm, with an uncertainty of about 10% (Halthore et al., 1997). The aerosol microphysical properties are calculated from sun and sky radiance measurements using the inversion algorithm of Dubovik and King (2000).

Sunphotometer measurements are limited in the extent of information which can be derived out of them. The inversion technique can not retrieve particles with a radius $r<0.05$ μm. Such small Aitken particles ($0.024<r<0.120$μm) and ultrafine particles ($0.004<r<0.014$μm) have been detected in the upper troposphere using airborne *in situ* measurements over the northern hemisphere (Minikin et al., 2003) during the INCA project in September-October 2000. Their composition and optical characteristics are not known, only their size distribution has been measured.

It is important to mention that the aerosol information obtained from sunphotometry is related to clear-sky conditions. Especially the sky radiance measurements, which are necessary to obtain aerosol microphysical information, can only be performed when no clouds are present at all. The aerosol microphysics data set is further reduced by the criteria imposed for the inversion retrieval technique as high aerosol loading, and large sun elevation angle.

*2.1.2. Data for the North Sea region*

Data on aerosol optical properties in the North Sea area are reported in the literature. Smirnov et al. (2002a) resumed shipborne measurements by sunphotometers taken in 1983, 1985 and 1997. The aerosol optical depth at 550nm, $\tau_a(550)$ was measured but the Ångstrom wavelength exponent is not available because just few filters were employed. The reported $\tau_a(550)$ values vary between 0.12 and 0.28. This is higher than open ocean conditions which are characterised by $\tau_a(550)$ values between 0.07 and 0.10 in the Pacific. Similar to the open ocean conditions are the background levels of aerosols defined by Holben et al. (2001) with $\tau_a(500)$ less than 0.10. Further shipborne measurements in this area (Hoyningen-Huene and Raabe, 1987) put in evidence the strong influence of the air mass origin on the aerosol optical depth and its spectral dependence.

Table 1. Aerosol optical properties calculated from sunphotometer data for coastal and urban northern European sites as well as two "maritime sites" from the northern hemisphere.

| Northern European island and coastal sites | **Helgoland, German Bight** 2000-2003, level 2 data April-September | **Oostende, Belgium** 2001-2003, level 2 data April-September |
|---|---|---|
| Number measurements (points) | 2403 | 4376 |
| Number of days | 163 | 232 |
| $\tau_a(500)$ min, max, median | $0.02 \le \tau_a(500) \le 0.9$, 0.185 | $0.03 \le \tau_a(500) \le 1.4$, 0.20 |
| $\tau_a(340)$ min, max, median | $0.07 \le \tau_a(340) \le 1.3$, 0.31 | $0.06 \le \tau_a(340) \le 1.7$, 0.33 |
| $\alpha_{440-870}$ min, max, median | $-0.02 \le \alpha \le 2.2$, 1.48 | $0.1 \le \alpha \le 3.1$, 1.48 |
| Number measurements ($\omega_0$, n, k) | 23 alm. (13 days) | 96 alm. (43 days) |
| n, min, max, mean | $1.33 \le n \le 1.57$, 1.42 ± 0.08 | $1.33 \le n \le 1.59$, 1.42 ± 0.07 |
| k, mean | 0.006 ± 0.002 | 0.006 ± 0.004 |
| $\omega_0$(440/670/870/1020) total | 0.95/0.93/0.91/0.89 ± 0.02 | 0.94/0.93/0.92/0.92 ± 0.01 |
| $\omega_0(550)$, min, max, mean | $0.93 \le \omega_0(550) \le 0.97$, ~0.95 | $0.88 \le \omega_0(550) \le 0.99$, ~0.94 |
| $r_{Vf}$ (μm); $\sigma_f$ | 0.12 + 0.1 $\tau_a(440)$ ; 0.46 ±0.04 | 0.14+0.04 $\tau_a(440)$ ; 0.46 ±0.07 |
| $r_{Vc}$ (μm); $\sigma_c$ | 2.14 + 1.8 $\tau_a(440)$ ; 0.84 ± 0.15 | 3.70 – 0.91 $\tau_a(440)$ ; 0.83 ± 0.1 |
| $C_{Vf}$ ($\mu m^3/\mu m^2$), mean | 0.047 + 0.04 $\tau_a(440)$, 0.073±0.02 | 0.013 + 0.11 $\tau_a(440)$, 0.079±0.02 |
| $C_{Vc}$ ($\mu m^3/\mu m^2$), mean | 0.068 ± 0.04 | 0.057 ± 0.04 |

| Northern European urban sites | **Hamburg, Germany** 2000,2003, lev2 ; 2002 lev1.5 April-September | **Lille, France** 2000-2001 lev2; 2002-2003 lev1.5 April-September |
|---|---|---|
| Number measurements (points) | 3584 | 5896 |
| Number of days | 186 | 322 |
| $\tau_a(500)$ min, max, median | $0.03 \le \tau_a(500) \le 0.9$, 0.205 | $0.04 \le \tau_a(500) \le 0.9$, 0.23 |
| $\tau_a(340)$ min, max, median | $0.07 \le \tau_a(340) \le 1.3$, 0.35 | $0.08 \le \tau_a(340) \le 1.4$, 0.39 |
| $\alpha_{440-870}$ min, max, median | $0.02 \le \alpha \le 2.7$, 1.54 | $0.3 \le \alpha \le 2.3$, 1.45 |
| Number measurements ($\omega_0$, n, k) | 52 alm. (22 days) | 41alm. (19 days) |
| n, min, max, mean | $1.33 \le n \le 1.6$ , 1.40 ± 0.07 | $1.33 \le n \le 1.58$ , 1.39 ± 0.09 |
| k, mean | 0.007 ± 0.004 | 0.008 ± 0.006 |
| $\omega_0$(440/670/870/1020) total | 0.94/0.93/0.91/0.91 ± 0.03 | 0.93/0.92/0.91/0.90 ± 0.06 |
| $\omega_0(550)$, min, max, mean | $0.86 \le \omega_0(550) \le 0.97$, ~0.94 | $0.78 \le \omega_0(550) \le 0.99$, ~0.93 |
| $r_{Vf}$ (μm); $\sigma_f$ | 0.13+0.07 $\tau_a(440)$ ; 0.46 ± 0.07 | 0.14+0.04 $\tau_a(440)$ ; 0.42 ± 0.05 |
| $r_{Vc}$ (μm); $\sigma_c$ | 2.68+1.07$\tau_a(440)$ ; 0.87 ± 0.12 | 3.47- 0.34 $\tau_a(440)$ ; 0.82 ± 0.12 |
| $C_{Vf}$ ($\mu m^3/\mu m^2$), mean | 0.021+ 0.11$\tau_a(440)$, 0.084 ± 0.02 | 0.012 + 0.14 $\tau_a(440)$, 0.086±0.03 |
| $C_{Vc}$ ($\mu m^3/\mu m^2$), mean | 0.045 ± 0.02 | 0.034+ 0.018 $\tau_a(440)$,0.044±0.03 |

| Northern European Maritime sites | **Rame Head, English Channel** 1997-1998, level 2 data April-September | **Azores, Atlantic Island** 2000-2003, level 2 data April-September |
|---|---|---|
| Number measurements (points) | 1264 | 3849 |
| Number of days | 88 | 237 |
| $\tau_a(500)$ min, max, median | $0.03 \le \tau_a(500) \le 0.62$, 0.125 | $0.02 \le \tau_a(500) \le 0.4$, 0.095 |
| $\tau_a(340)$ min, max, median | $0.05 \le \tau_a(340) \le 0.67$, 0.175 | $0.04 \le \tau_a(340) \le 0.5$, 0.14 |
| $\alpha_{440-870}$ min, max. median | $0.05 \le \alpha \le 2.2$, 1.27 | $0 \le \alpha \le 2.2^{**}$, 0.97 |
| Number measurements ($\omega_0$, n, k) | none | none |
| n; k, $\omega_0$(440/670/870/1020) | No retrieval | No retrieval |
| $r_{Vf}$ (μm) $r_{Vc}$ (μm) ; $C_{Vf}$; $C_{Vc}$ | No retrieval | No retrieval |

** the maximum value of the $\alpha_{440-870}$ is calculated for $\tau_a(500) \ge 0.1$ values, related to the ground based conditions

In the framework of AERONET, several sunphotometers have been installed also in the vicinity of the German Bight. The Institute for Coastal Research of GKSS, Geesthacht, Germany is operating a CIMEL sunphotometer on Helgoland Island (N 54°10', E 07°53', Alt 33 m). This island is about 1km$^2$ large and is located at about 70km from land, in the middle of the German Bight, directly in the region of interest for the MERIS data evaluation. The available sunphotometer data are listed in Table 1. Two data sets are distinguished:

(1) sun radiance measurement points (a point is related to a triplet of direct sun measurement made over each available spectral band) and measurement days from which the spectral aerosol optical depth, Ångström wavelength exponent and the water vapour content is calculated and

(2) sun and sky-radiance (almucantar) measurements which fulfil the inversion technique criteria and from which the refractive index, single scattering albedo and particle size distribution parameters can be determined. The asymmetry parameter is not considered here.

The second data set is included in the first one but it is significantly smaller because of the higher demands for clear sky conditions. Thus it covers only 10% of the total days.

AERONET data from three other North Sea coastal sites (Hamburg, Oostende and Lille) at increasing distances from the region of interest, the German Bight, are used to investigate the distribution of the aerosol properties in this area (Fig.1). Two additional stations, one in the eastern part of the Atlantic Ocean (Azores) and one at the Atlantic coast of England (Rame Head) were chosen as reference data sets. Azores represent clean maritime conditions while Rame Head is expected to be only slightly influenced by European pollution. Due to the standardisation of the data processing algorithms and the calibration procedure, aerosol data from different sites can be compared and aerosol regional distributions can be established (Holben et al., 1998). The five sites can be briefly described as follows:

a) Hamburg (N 53°34', E 09°58', Alt 105 m) is a 1.7 million habitants town, situated in a flat terrain at about 70 km from the coast. The instrument is operated on top of a high building in the city center.

b) Lille (N 50°36', E 03°08', Alt 60 m) is also situated about 70 km from the sea. It is a densely populated town with 1 million habitants living in the Lille area. A lot of industry can be found in the neighbouring area.

c) Oostende (N 51°13', E 02°55', Alt 23 m) is a port city situated on the Belgium coast at about 100 km from Lille. The area is industrialised and densely populated, but Oostende itself has only 70000 habitants.

Figure 1. Map with the selected AERONET sites: Helgoland, Hamburg, Oostende, Lille, Rame Head and Azores

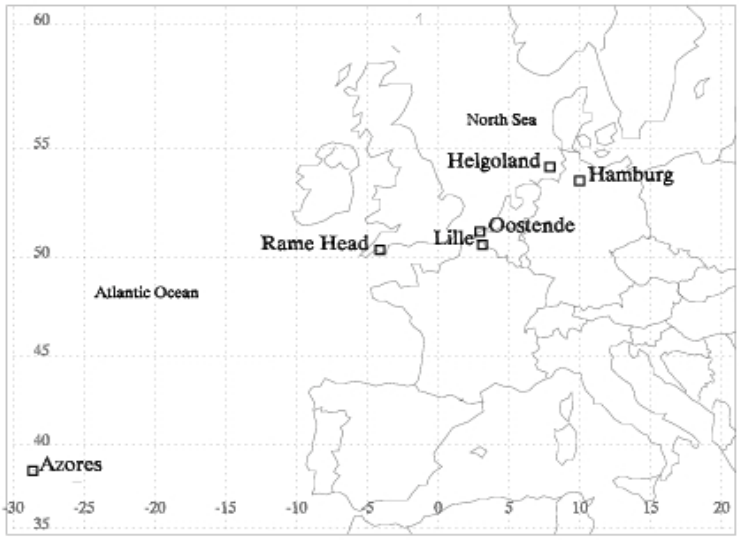


d) Rame Head (N 50°21', W 04°08', Alt 0 m) is located on the English Channel coast. It is a low populated area, with a 220° panorama of the sea. Due to the prevailing SW winds, this site receives mainly air masses with marine origin. This site is chosen as a reference for a clean maritime site, which is occasionally influenced by European continental air masses.
e) Azores Islands (N 38°31', W 28°37', Alt 50 m) are located in the Atlantic Ocean, at about 5000 km west off the Portuguese coast. This site is used as a reference for the maritime aerosol type from the northern hemisphere. However, Saharan dust storms are occasionally present over the Atlantic Ocean (Carlson and Prospero, 1972; Kaufmann et al., 2001a).

The sunphotometer is operating mainly during the summertime at Helgoland (April-September). This coincides with the alga blooming period in the North Sea area with maximum growth rates during the months of April and August. The phytoplankton quantification from MERIS imagery is done mainly during this period. Differences of the aerosol optical properties for winter (October-March) and summer (April-September) have been established on the basis of lidar measurements over Hamburg (Matthias and Bösenberg, 2002). The statistics and the comparison of the AERONET data from all sites is documented here for the summer periods of 2000-2003.

### *2.2. Raman Lidar*

#### *2.2.1 Methods*

Raman lidar measurements were used to derive vertical profiles of the aerosol extinction coefficient. The Raman lidar technique (Ansmann et al., 1992) allows the determination of aerosol extinction profiles without assumptions on the extinction to backscatter ratio (lidar ratio) and without the need for calibration of the lidar signal in an aerosol free region. Therefore, Raman lidars can give more accurate aerosol extinction profiles than pure backscatter lidars, which always rely on the unknown lidar ratio. The measurements require low solar background conditions and are usually taken at sunset. At this time the planetary boundary layer (PBL) is still fully developed and the aerosol remains well mixed in the PBL. The planetary boundary layer height can be derived from significant gradients in the aerosol profile. This methods has been used since long time in the lidar community (e.g. Russell et al., 1974; Coulter, 1979; Menut et al., 1999). It delivers accurate values of the PBL height with typical spatial resolutions of a few dm.

The error of the aerosol extinction coefficient depends on averaging time and vertical averaging length. It is typically in the order of 10–20 % or less than 0.05 1/km. The aerosol optical depth can be calculated as integral of the aerosol extinction with a typical error of 20 % or 0.05. Here, additional errors are caused by the assumption of constant aerosol extinction in the lowest few hundred meters of the atmosphere, where the lidar cannot deliver extinction values. Comparisons with sun and star photometers (Ansmann et al., 2001; Matthias and Bösenberg, 2002) and with other lidar systems (Matthias et al., 2004a) confirm this error estimation.

*2.2.2 Data set*

The data used for the aerosol climatology was taken on a regular schedule between January 1998 and August 2003 in Hamburg. During this time the Aerosol Raman Lidar of the Max-Planck-Institut für Meteorologie was part of the German aerosol lidar network (1998 – 2000) (Bösenberg et al., 2001) and of EARLINET (European Aerosol Research Lidar Network, 2000 - 2003) (Bösenberg et al., 2003). In 1998 and 1999 measurements were taken once a week (each Monday), since 2000 they were taken twice a week (each Monday and Thursday). All measurements are taken at UV wavelengths (351 nm or 355 nm).

The whole data set from Hamburg comprises 193 vertical aerosol extinction profiles, typically 30 min averages with a typical vertical resolution of 240 m. Because the aerosol extinction from Raman lidar can also be derived under cloudy conditions, about 12 % of the measurements were taken under conditions with clouds below 2000 m altitude. In these cases, the aerosol optical depth can only be determined up to the cloud base. About 70 % of the measurements reach altitudes of 5000 m or more.

*2.3. Meteorological data*

The aerosol types, their concentrations and their optical properties depend on the air mass origin and on the processes the aerosols have undergone on their way to the measurement site. A synoptic air mass analysis is recommended by Smirnov et al. (1994; 1995) in order to determine the atmospheric optical characteristics related to different air mass types. The authors proposed an application of this method to the atmospheric correction algorithms, where the aerosol optical properties could be estimated a priori on the base of the synoptic charts without in situ related atmospheric measurements.

Synoptic charts at 850 hPa pressure level (1.5 km height) from 00 UT over Europe and synoptic surface charts at 12UT over Central Europe are calculated by the Meteorological Institute of the Free University Berlin (http://wkserv.met.fu-berlin.de/) on a daily basis. The synoptic air mass type is established after its origin, the back trajectory information and the whole heat content of the air mass measured by radiosondes at 850hPa. In wintertime, when the mixed layer depth frequently stays below a few hundred meters, the values at 950hPa are taken (Geb, 1971; Vogt, 2000). The following air mass classes are defined for central Europe: arctic, subpolar, warmed subpolar, middle latitude and subtropical. Each of these classes has maritime or continental character, depending on the circulation pattern. The air mass which flows equally over maritime and continental regions before reaching the measurement point is called “modified”, because it has both characters.

The sunphotometer on Helgoland Island delivered AERONET-level 2 data on 163 days between 2000 and 2003, with measurements mostly taken around noon. In order to establish links between the synoptic air masses and the optical properties ($\tau_a(500)$, $\alpha_{440-870}$ and PW) of the aerosols the surface synoptic charts at 12UT are employed.

## 3. Statistical methods

The optical depth at 500 nm ($\tau_a(500)$) is used as a parameter in the radiative transfer simulations since this wavelength corresponds to the maximum of the solar irradiance. The sunphotometers at Lille, Rame Head and Hamburg (2000) are not equipped with this channel. Then, $\tau_a(500)$ is determined from adjacent values of $\tau_a(440)$ and $\tau_a(670)$ using the equal weighting method as follows:

$$\tau_a(500) = \frac{670-500}{670-440}\tau_a(440) + \frac{500-440}{670-440}\tau_a(670)$$

The $\tau_a(340)$ values is also evaluated and compared between sites because they are close to the lidar wavelength (355 nm) used at Hamburg site. This band is not specific for the sunphotometers from Hamburg (2000), Lille and Rame Head and the $\tau_a(340)$ is calculated by extrapolation from $\tau_a(440)$ using the Ångström wavelength exponent between 440 and 870nm, $\alpha_{440-870}$.

### *3.1 Frequency distributions*

It has been shown previously (O'Neill et al., 2000; Matthias and Bösenberg, 2002) that the frequency distribution of the aerosol optical depth $\tau$ follows a log normal distribution,

$$f(\tau) = \frac{1}{s\tau\sqrt{2\pi}}\exp\left(\frac{(\ln\tau - m)^2}{2s^2}\right)$$

which means that ln $\tau$ follows a Gaussian (or normal) distribution with the mean *m* and the standard deviation *s*. The median of the distribution is then given by *median* = exp(*m)*. Therefore the median describes the average conditions much better than the mean does and it will be used in this study for comparison of the individual stations. The use of medians instead of means is also recommended by Kaufman et al. (2001b) in order to decrease the contribution of rare cases of dust and pollution, which could be present at a maritime site, to the parameters characterising the site.

The lognormal distribution is used here for all measurement points or the daily means. A comparison between all sunphotometer measurement points and the daily means of $\tau_a(500)$ for the Helgoland during 2000-2003 demonstrates high similarities between the two types of data (Table 2). The $\tau_a(500)$ daily mean and the related median of the distribution is considered further for statistical purposes because it is more representative.

Table 2. Helgoland island, $\tau_a(500)$ and $\alpha_{440-870}$ level2 data 2000-2003 summertime (April-September), characteristics of the lognormal distribution that fit best to the measured values, N=number of independent values, m=mean of the distribution, σ=standard deviation of the mean, median=median of the distribution, s=standard deviation of the distribution .

| | N | m | σ | median | s |
|---|---|---|---|---|---|
| $\tau_a(500)$ all points | 2403 | 0.224 | 0.135 | 0.190 | 0.574 |
| $\tau_a(500)$ daily means | 163 | 0.221 | 0.139 | 0.187 | 0.577 |
| $\alpha_{440-870}$ all points | 2403 | 1.46 | 0.44 | 1.57 | - |
| $\alpha_{440-870}$ daily mean | 163 | 1.37 | 0.44 | 1.48 | - |

No typical frequency distributions of the Ångström wavelength exponent which would be expected at the sites under investigation have been reported up to now. The frequency distributions are not fitted by analytic functions.

*3.2.Correlation analysis*

The correlation analysis looks for similarities in the temporal distribution of the aerosol optical depth at Helgoland and the other AERONET sites. $\tau_a(\lambda)$ daily mean values are taken for this correlation study. Common measurement days of the lidar in Hamburg and the sunphotometer in Hamburg (23 common days) and Helgoland (34 common days) are used to look for correlation between the $\tau_a(340)$ values obtained by two different techniques in the same place or at two different sites.

## 4. Results

The whole sunphotometer data set is subdivided into three different data sets. One contains all data points, one contains daily means and the third, very limited, data set consists of microphysical retrievals from almucantar measurements. For the aerosol optical depth and the Ångström wavelength exponent, the results for all data points and for daily mean values are presented. All available almucantar measurements are taken for the statistics of the microphysical aerosol properties.

*4.1. Aerosol optical depth*

*4.1.1. Diurnal cycle at Helgoland*

MERIS has a daily overpass for the German Bight at about 10:30 UT and the atmospheric correction has to consider the atmospheric parameters specific for this time. Urban/industrial areas, like northern Europe, are characterised by a diurnal variability of the aerosol optical depth, with maximum reached in the afternoon (Smirnov at al., 2002b). A comparison between average $\tau_a(500)$ values in the timeframe from 9:30 to 11:30 UT and the related $\tau_a(500)$ daily means, shows a correlation factor of about 0.98 for 79 days at Helgoland site (Fig.2). The data set can be considerably expanded if daily means are taken for this statistics and they are considered to be representative for the aerosol optical depth at the overpass time.

Figure 2. Correlation between the aerosol optical depth at 500nm, $\tau_a(500)$ averaged over the 9-11 UT values and the $\tau_a(500)$ daily mean for the Helgoland site, with R correlation coefficient.

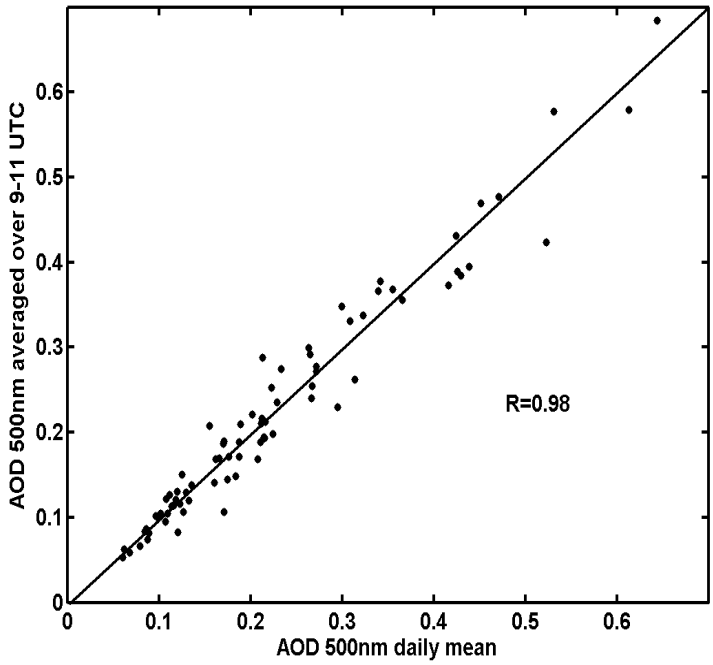


*4.1.2 Frequency distribution and median values*

The statistical evaluation (see Table 3) shows a large skewness, larger than 1, for all data sets. As expected (O'Neill et al., 2000; Matthias and Bösenberg, 2002) the lognormal distribution is well followed by all data sets. The values for *median* and *s* which represent the measured distributions can also be seen in Table 3. Additional to the 500 nm value, measurements at 340 nm wavelength are also considered.

Table 3. Statistics of daily means of $\tau_a(340)$ and $\tau_a(500)$ for the summertime period (April – September) of 2000-2003 (1997-1998 Rame Head). N=number of days, m=mean, σ=std.dev., γ=skewness, median, s=std.dev.(on log scale), 16%- and 84%-percentiles.

| AERONET site | N | m | σ | γ | 340nm median | s(log) | 16%-perc. | 84%-perc. |
|---|---|---|---|---|---|---|---|---|
| Helgoland | 163 | 0.345 | 0.20 | 1.30 | 0.31 | 0.55 | 0.165 | 0.510 |
| Hamburg | 186 | 0.398 | 0.23 | 1.20 | 0.35 | 0.57 | 0.190 | 0.615 |
| Oostende | 232 | 0.397 | 0.24 | 1.71 | 0.33 | 0.55 | 0.190 | 0.610 |
| Lille | 322 | 0.439 | 0.27 | 1.66 | 0.39 | 0.58 | 0.190 | 0.675 |
| Rame Head | 88 | 0.236 | 0.17 | 1.47 | 0.175 | 0.60 | 0.110 | 0.395 |
| Azores | 237 | 0.163 | 0.08 | 1.24 | 0.14 | 0.46 | 0.095 | 0.200 |
| AERONET site | N | m | σ | γ | 500nm median | s(log) | 16%perc. | 84%perc. |
| Helgoland | 163 | 0.221 | 0.14 | 1.43 | 0.185 | 0.58 | 0.105 | 0.345 |
| Hamburg | 186 | 0.236 | 0.14 | 1.42 | 0.205 | 0.60 | 0.105 | 0.355 |
| Oostende | 232 | 0.252 | 0.17 | 2.10 | 0.200 | 0.58 | 0.120 | 0.390 |
| Lille | 322 | 0.268 | 0.16 | 1.66 | 0.230 | 0.55 | 0.130 | 0.420 |
| Rame Head | 88 | 0.157 | 0.10 | 1.32 | 0.125 | 0.55 | 0.085 | 0.250 |
| Azores | 237 | 0.114 | 0.06 | 1.12 | 0.095 | 0.51 | 0.060 | 0.180 |

The highest median values for $\tau_a(500)$ are found at Lille (0.23). At Hamburg and Oostende the values are slightly lower (0.205 and 0.20) and the median at Helgoland is with 0.185 again somewhat lower. However, the differences between these stations are only 20 %, while the median at Rame Head is significantly lower (0.125) and at Azores even background conditions (0.095) can be found (Smirnov et al., 2002a; 2003). The aerosol optical depth at Helgoland is much closer to values in an urban environment along the North Sea coast than to pure maritime sites or clean coastal sites. Thus it has to be classified as an urban maritime site.

The range of most likely values is given by the 69 % interval around the median. This interval is very similar for Hamburg and Helgoland (approx. 0.1-0.35), Oostende and Lille exhibit somewhat higher values (0.12 –0.39 and 0.13 – 0.42), but the differences are not large. At Azores, the narrowest distribution can be found while Rame Head is much closer to Azores than to the North Sea coastal sites (see Table 3).

Comparing the daily means from Table 3 to the statistics of all points, no large differences were observed. At three of the stations (Hamburg, Lille and Azores) the median of all points was up to 5% lower than that of the daily means, at the other three stations (Helgoland, Oostende and Rame Head) it was up to 10 % larger. Averaged over all stations the difference between the data sets given by the median of $\tau_a(500)$ is 1.3 %.

*4.1.3. Annual cycle*

The large temporal variability of the aerosol optical properties is well connected with different meteorological conditions. This has been shown on the basis of a synoptic air mass analysis (Smirnov et al., 1995). Also a seasonal variability for the northern mid-latitude regions is mentioned by different authors (Holben et al., 2001; Matthias and Bösenberg; 2002). The seasonal cycles of $\tau_a(500)$ have a maximum during the summertime, the mid latitude air mass circulation slows down and aerosols can accumulate in the planetary boundary layer. Helgoland, Oostende, Hamburg and Lille present this peak of $\tau_a(500)$ during the period of July-August (Fig. 3). This aerosol optical depth peak is associated with the highest monthly means of the Ångström, between 1.55 and 1.7 (Behnert et al., 2004), which confirms the presence of high concentrations of urban aerosols at this time. The Azores site shows no seasonal peaks as expected for a maritime station with mostly sea salt aerosols. Rame Head shows no clear peaks during the one and a half year observation period. This result might have been caused by the stronger Atlantic influence at this site compared to the others. However, the few available data make a reliable interpretation difficult.

An additional springtime maximum during April-May is present at Helgoland, Oostende, Hamburg and Lille and is missing at the other two sites. The springtime peak was observed at several AERONET sites from the Atlantic islands (Kaufman et al., 2001b) but not explained. Regular measurements of the aerosol extinction by Raman lidar over Hamburg, Kühlungsborn and Leipzig, all German stations, show the same seasonal cycle (Matthias et al., 2004b). The reason for this is not yet clear. A possible explanation is the influence of the high relative humidity during springtime, causing hygroscopic growth of the aerosol particles. The particle growth produces the decrease of the Ångström wavelength exponent. At all four sites, this aerosol optical depth peak is not associated with a visible decrease of the Ångström. Special circulation patterns in central and northern Europe are also under investigation to explain the annual cycle of the aerosol optical depth.

Figure 3. Seasonal variability of the aerosol optical depth at 500nm, $\tau_a(500)$ at the northern Europe AERONET sites, monthly averages. The inner error bars are the standard deviation of the average (standard error) and the outer bars are the standard deviation of the individual value.

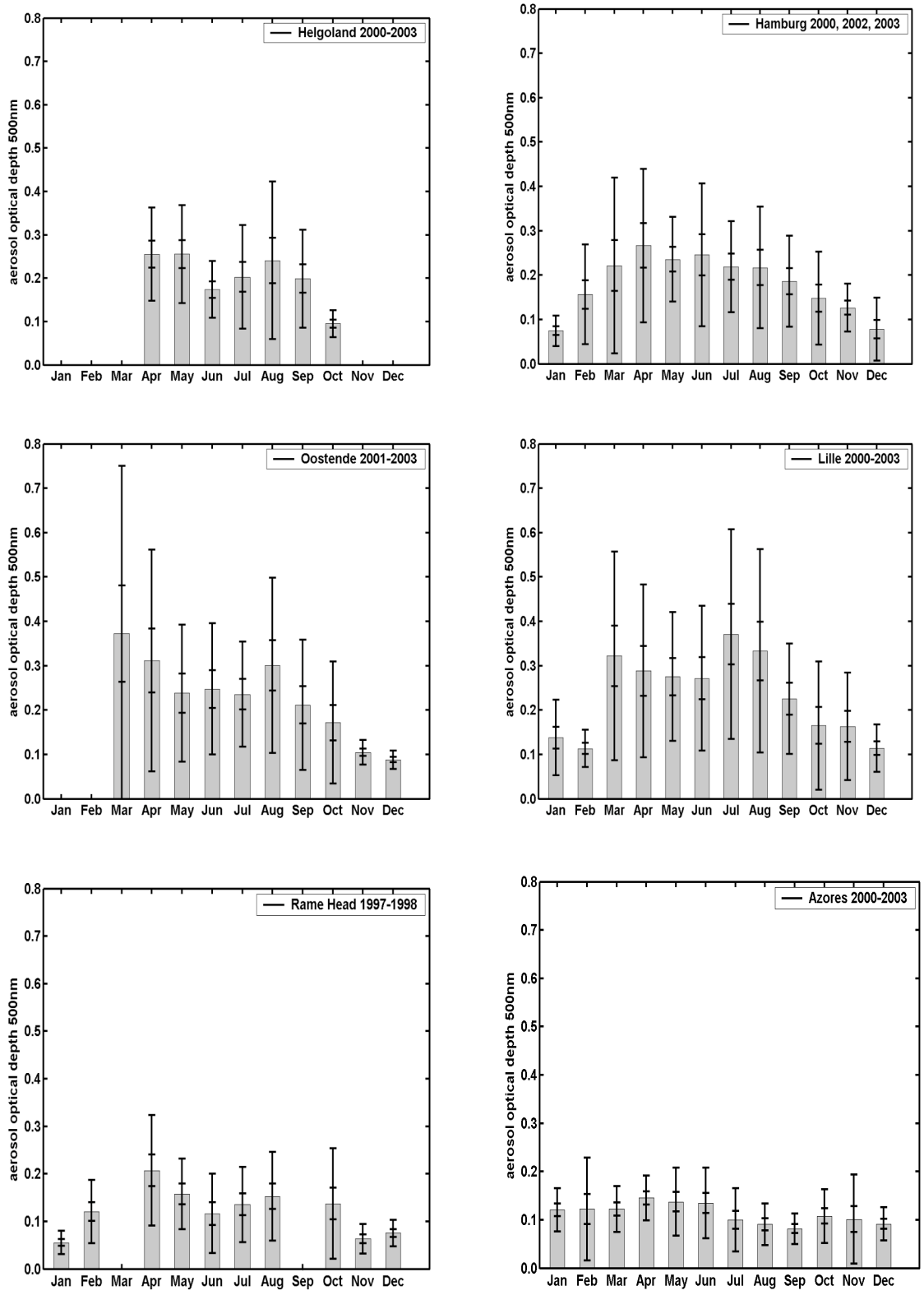

*4.1.4. Correlation analysis*

A correlation analysis (Behnert et al., 2004) of only common measurement days of Helgoland, Hamburg, Oostende, Lille and the Azores demonstrates that the Helgoland $\tau_a(500)$ data is correlated with that from Hamburg showing a correlation coefficient of 0.61. The correlation decreases with increasing distance from the site, where Helgoland and the Azores are not correlated at all.

The correlation between the Helgoland and Hamburg sites is also reflected in the lidar measurements (Fig 4). At Hamburg, the aerosol optical depth in the UV can be derived from the CIMEL sunphotometer and the Raman lidar. An analysis of the $\tau_a(340)$ values on common measurement days shows a correlation between the lidar and the sunphotometer measurements, although the Raman lidar data can only be taken after sunset, which is typically 2–3 hours after the last sunphotometer measurement. Taking only the data from 2003, the correlation coefficient is 0.89 and the mean values of $\tau_a(340)$ are almost equal at

Figure 4. Correlation of the $\tau_a(355)$ measured by lidar in Hamburg with the sunphotometer $\tau_a(340)$ measured in Hamburg and Helgoland for 2000-2003.

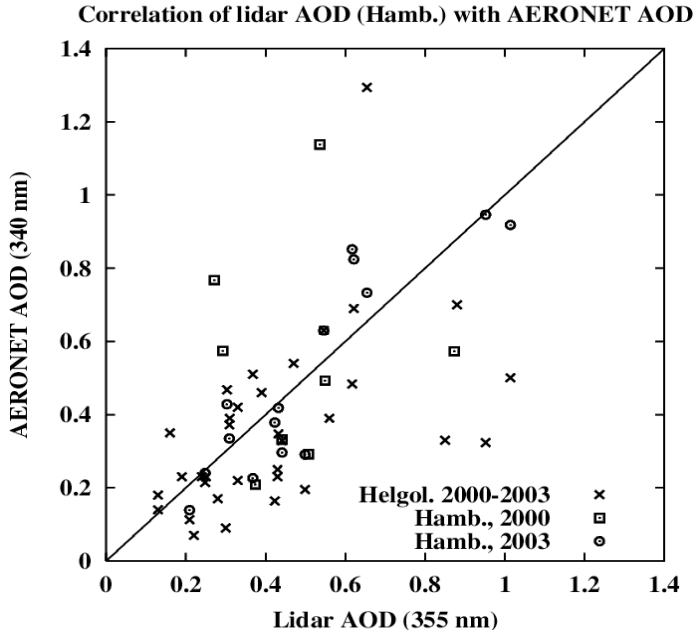


0.51. The correlation was not that high in 2000 (2000 was the first year of common measurements) reducing the total correlation for both years to 0.63 and introducing a discrepancy in the mean values (0.52 from the sunphotometer, 0.49 from the lidar). This shows that the optical depth values from lidar are consistent with the sunphotometer measurements and that the lidar gives accurate $\tau_a$ values although the troposphere is not completely covered by the measurements. Despite the distance of approx. 100 km, the lidar aerosol optical depth in Hamburg correlates also well with the sunphotometer measurements from Helgoland (correlation coefficient 0.51 in the 2000 – 2003 period), therefore the lidar profiles are considered to be representative in a larger area around Hamburg, that covers also the region of interest for the MERIS evaluation, the southern North Sea.

*4.2.Ångström wavelength exponent*

The frequency of occurrence of the Ångström wavelength exponent between 440 and 870 nm, $\alpha_{440\text{-}870}$ is studied for each site for summertime. The statistics including all measurement points (bars) and daily means (lines) can be seen in Fig. 5.

All AERONET sites with the exception of Azores present a mode with $\alpha$ values of approx. 1.7, which is related to small particles. Another mode is characterised by $\alpha$ values of approx. 0.9 related to larger aerosols (maritime or maritime-polluted), present at Helgoland and Rame Head. Similar $\alpha$–mode values ranging between 0.7 and 0.9 are reported by Smirnov et al. (2002a; 2003) for Bermuda and Ascension (Atlantic Ocean).

The range of $\alpha$ values at the Azores with no maximum indicates a wide range of particle sizes. Sea salt aerosols and Saharan dust are associated with low $\alpha$ values representing the large size of the particles. The presence of dust is confirmed by the fact (Holben at al., 2001), that the largest $\tau_a(500)$ values correspond to the lowest $\alpha$ values. Continental aerosols with Ångström wavelength exponents larger than 1.3 are observed in less than 10% of the cases.

All other sites show larger values of the median, between 1.45 (Lille) and 1.54 (Hamburg), see Table 4. With a median of 1.48 Helgoland is within this range. Smaller values are somewhat more frequent at Helgoland, the 16% percentile is 0.88 while it is 1.09 at Hamburg and Lille and 1.15 at Oostende. However, large values of the Ångström exponent are most frequent at Helgoland, the 84 % percentile is 1.84, somewhat larger than the values at Hamburg and Oostende (1.81) and Lille (1.72). Helgoland shows the widest distribution of values, indicating the mixture of maritime and urban aerosols present at this site.

The statistics of the daily means exhibits slightly lower values (5-10 %) of the Ångström wavelength exponent compared to all data points (Fig. 5). The reason for this is the overrepresentation of clear sky days with a high number of measurements (they are taken every 15 minutes) in the statistics of all measurements. Shallow convection developing in the course of the day often only allows measurements in the morning and the evening. Fig. 6 shows that at all stations the daily mean of the Ångström coefficient is increasing with the number of measurements per day. This can have several reasons: Humidity effects in the morning and evening lead to larger aerosol particles and therefore lower Ångström wavelength exponent. So on days, which are only cloud free in the morning and evening hours, the mean measured Ångström coefficient will be biased towards lower values. The daily variability of the size distributions of the urban/industrial aerosols within changing values of the relative humidity was considered also by other authors (Remer and Kaufman, 1998; Eck et al., 1999). Additionally, clear sky days are often associated with a significant accumulation of urban aerosols in the PBL, leading to high Ångström wavelength exponents of the small dry particles.

Figure 5. Frequency of occurrence of Angstrom wavelength exponent, $\alpha_{440-870}$ on base of AERONET summertime data, considering all measurement points (bars) and the daily means (dashed line).

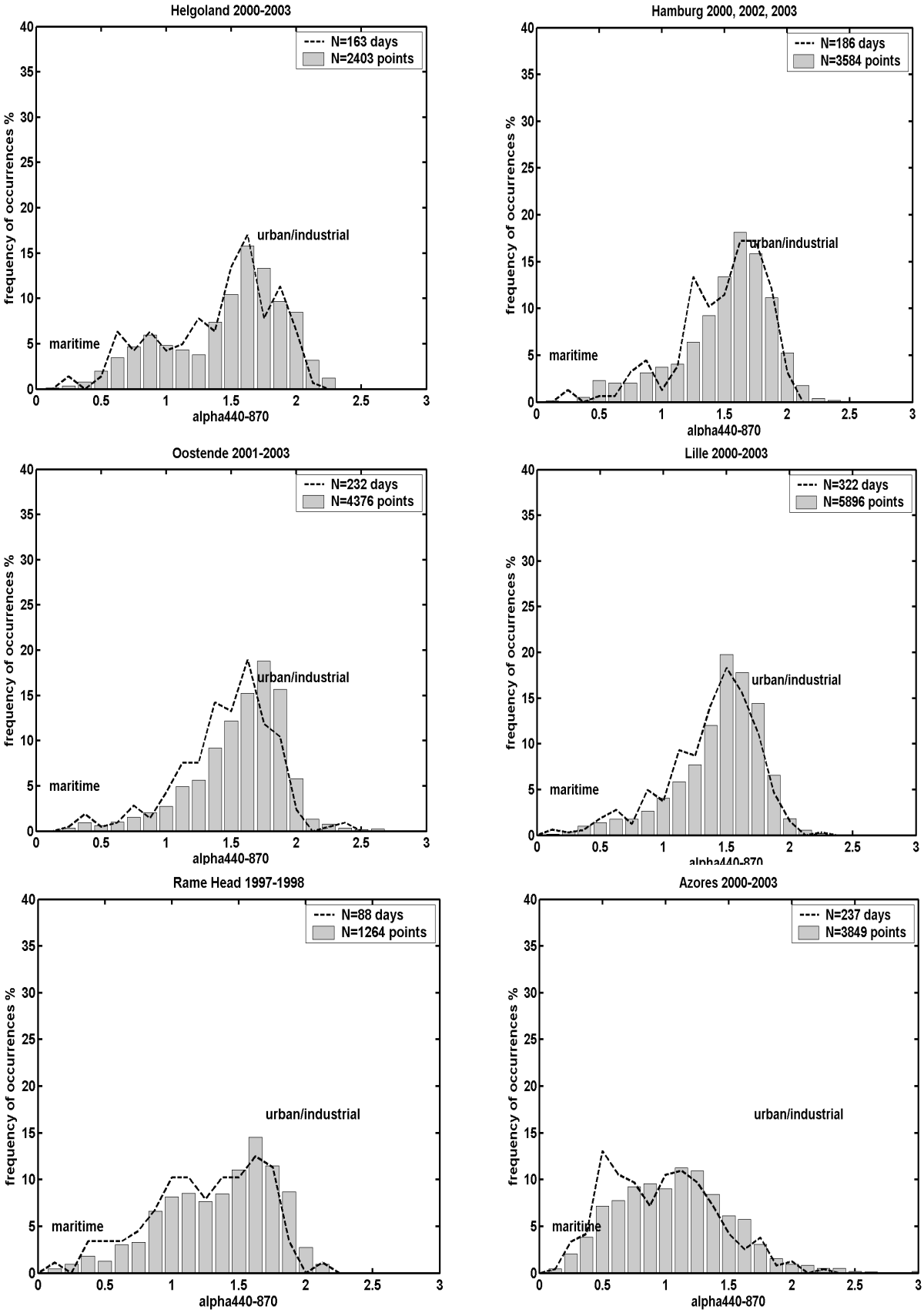

Table 4. Statistics of daily means of $\alpha_{440-870}$ for the summertime (April – September) of 2000-2003 (Rame Head 1997-1998). N=number of days, m=mean, σ=std. dev., γ=skewness, median, s=std. dev. (on log scale), 16%- and 84%-percentiles.

| AERONET site | N | m | σ | γ | 440/870nm median | s(log) | 16%perc. | 84%perc. |
|---|---|---|---|---|---|---|---|---|
| Helgoland | 163 | 1.37 | 0.44 | -0.49 | 1.48 | 0.41 | 0.88 | 1.84 |
| Hamburg | 186 | 1.45 | 0.37 | -0.87 | 1.54 | 0.34 | 1.09 | 1.81 |
| Oostende | 232 | 1.45 | 0.37 | -0.71 | 1.48 | 0.34 | 1.15 | 1.81 |
| Lille | 322 | 1.38 | 0.35 | -0.90 | 1.45 | 0.35 | 1.09 | 1.72 |
| Rame Head | 88 | 1.24 | 0.42 | -0.41 | 1.27 | 0.44 | 0.82 | 1.66 |
| Azores | 237 | 0.96 | 0.42 | 0.42 | 0.97 | 0.51 | 0.52 | 1.39 |

Figure 6. The mean of the Angstrom wavelength exponent calculated from the daily means values depends on the number of available measurements during the day, the error bars are the standard deviation of the average (standard error).

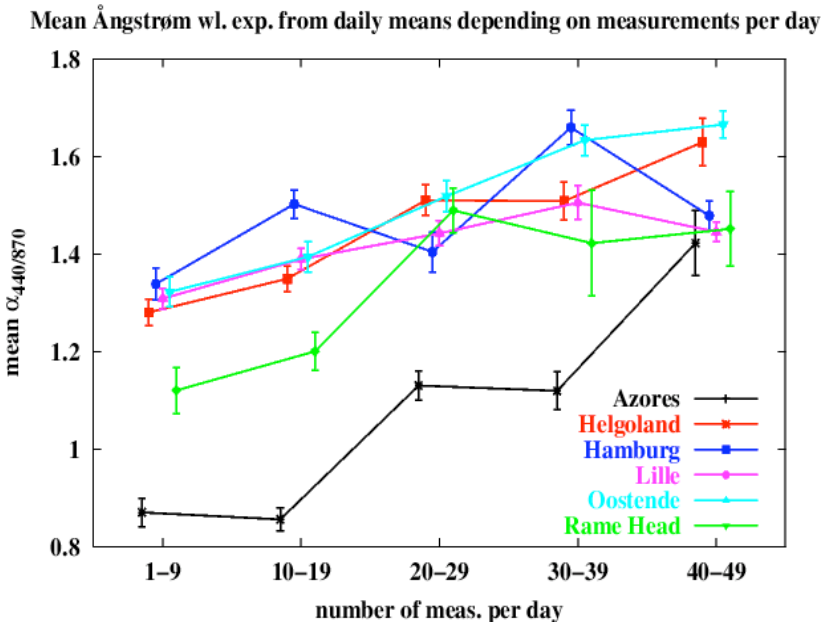


*4.3.Single scattering albedo*

The single scattering albedo $\omega_0(\lambda)$ is the appropriate parameter to express the relationship between scattering and absorption of aerosols (Kaufman et al., 1997; Dubovik et al., 2002). The averaged values of $\omega_0(\lambda)$ at 440, 670, 870 and 1020 nm are compared between Helgoland, Hamburg, Oostende and Lille. The retrieved values of $\omega_0(\lambda)$ are calculated for the total mode and are reported in Table 1. No retrievals exist for Rame Head and Azores due to the low aerosol loading.

The average value of the total mode of $\omega_0(\lambda)$ related to the four sites are represented in Fig. 7. Helgoland shows the highest value for $\omega_0(550)$ (~0.95), but at Hamburg, Oostende, ($\omega_0(550)$~0.94) and Lille, ($\omega_0(550)$~0.93) comparable values are found. Maritime sites as Lanai, Bermuda and Kaashidoo are characterised by values of $\omega_0(550)$~0.98 (Smirnov et al., 2003), the influence of polluted air masses at Helgoland is again demonstrated. Comparable values are also reported for Paris, $\omega_0(550)$~0.94-0.93 (Dubovik et al., 2002). Taking into

account the uncertainties of the $\omega_0$-values, no differences between the sites can be found in the current data set.

Figure 7. Single scattering albedo (total mode) for Helgoland, Hamburg, Oostende, Lille, 2000-2003 summertime.

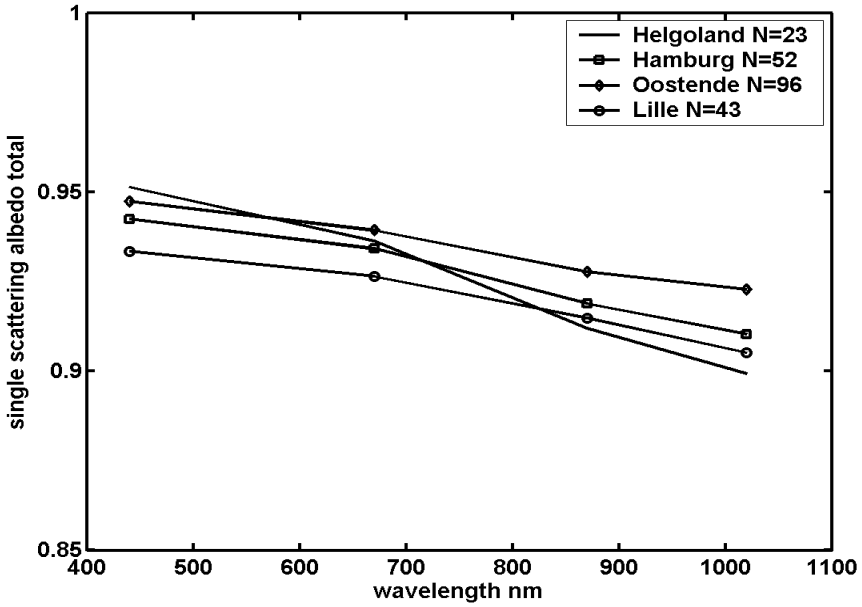


*4.4. Index of refraction*

The mean value of the refractive index found at Helgoland and Oostende (Table 1) is identical, with values of n(550)=1.42 and it shows lower values of n(550)=1.39-1.40 for Hamburg and Lille. The differences between the sites remain small, they are similar to those reported for Paris and Greenbelt (n(550)=1.40-1.41, Dubovik et al., 2002). No spectral dependence for the retrieved real part of the refractive index is observed at Helgoland and Oostende sites. This feature is found also at other islands sites (Smirnov et al., 2003), but here lower values of n=1.37 are reported. A weak spectral dependence is present at Hamburg and Lille, but the error margins do not allow to draw further conclusions from this.

*4.5.Particle size distribution*

The parameters of the particle size distribution using a bimodal lognormal distribution are reported for the different sites in Table 1. The particle volume concentration $C_{Vi}$ and the median radius $r_{Vi}$, i denoting the different modes (fine and coarse), increases with $\tau_a$ and can be parameterized using a linear relationship. At Helgoland, the total volume of the fine mode particles $C_{Vf}$~0.073 $\mu m^3/\mu m^2$ is approximately equal to the total volume of the coarse mode $C_{Vc}$~0.068 $\mu m^3/\mu m^2$, no mode dominates. The situation is changing for the other sites, where the total volume of the fine particles becomes larger than the volume of the coarse particles. At Oostende $C_{Vf}/C_{Vc}$ is about 1.4, at Hamburg about 1.8 and at Lille a value of approx. 2 is found.

The scattering of light by fine particles dominates between 440 and 1020 nm, which is the spectral region used for the retrieval, and becomes stronger for higher aerosol loading levels. The total volume of the fine particles increases with $\tau_a(440)$ by a factor of 0.11-0.14 for these

3 sites. The total volume of the coarse particles is almost independent of $\tau_a(440)$ for most of the sites with the exception of Lille where $C_{Vc} = 0.034 + 0.018\ \tau_a(440)$.

The mean value of the median radius in the coarse mode is 3.14±1.13 μm for Helgoland, 3.18±0.77 μm for Oostende, 3.28 ± 0.56 μm for Hamburg and 3.28 ± 0.65 μm for Lille. The mean value of the median radius related to the fine mode is about 0.17 for all four sites.

The data for island sites with maritime conditions ($\tau_a(500)<0.15$ and $\alpha<1$) is characterized by average values of $r_{Vc}$ between 2.44 and 2.78 (Smirnov et al., 2003). The "maritime conditions" occur very seldom at the northern European sites, but they are related to similar averaged values of $r_{Vc}$ for Helgoland (2.72, N=4), Oostende (2.74, N=24), Hamburg (2.33, N=3) and Lille (2.35, N=21).

Other reported values (Dubovik et al., 2002) at an urban-industrial site as Greenbelt/Maryland are: $r_{Vc}$~3.0 μm and $r_{Vf}$ ~0.15-0.17 μm for an aerosol loading related to $\tau_a(450)$ between 0.5 and 0.6. For this aerosol loading the mean values of $r_{Vc}$ are 3.7 μm at Helgoland, 3.3 μm at Hamburg, 3.2 μm at Oostende and 2.96 μm at Lille. The fine mode mean value of $r_{Vf}$ is for Helgoland 0.16 μm, Hamburg 0.17 μm, Oostende 0.17 μm and Lille 0.18 μm. The coarse mode of Lille is similar to that retrieved at Greenbelt/Maryland. At the other sites this mode is characterized by higher values of $r_{Vc}$ caused by maritime aerosols. The fine mode values are comparable between Greenbelt and these northern European AERONET sites.

From all the sites, Helgoland has the most pronounced increase of the median radius with $\tau_a(440)$ in the fine mode. The slope is similar to that found at Greenbelt and Paris in the fine mode. The higher levels of relative humidity related to an island could be responsible for a hygroscopic growth of the fine particles as other authors mentioned (Shettle and Fenn, 1979; Dubovik et al., 2002).

### *4.6.Vertical extinction profiles*

The lidar data shows that the vertical distribution of aerosols can be very different from day to day. Fig. 8 shows the annual cycle of the PBL heights determined with the Aerosol Raman Lidar at Hamburg between 1998 and 2003. On average, it follows a sine function with the highest values around 1 July and the lowest around 1 January. Nevertheless, the individual PBL heights can differ significantly from day to day and also the amount of aerosols in this lowest layer can be quite variable. In most cases about 80 % of the aerosol optical depth is caused by aerosol in the PBL (Matthias et al., 2004b). However, aerosol is also transported in upper layers, where it can persist for several days and can be transported several thousand of kilometres (Papayannis et al., 2004; Ansmann et al., 2003; Bösenberg et al., 2003). By this, Saharan dust can also be transported to the North Sea area, but these events are rare and can only be observed 1-3 times per year.

Figure 8. Annual cycle of the PBL over Hamburg from regular lidar measurements (1998-2003).

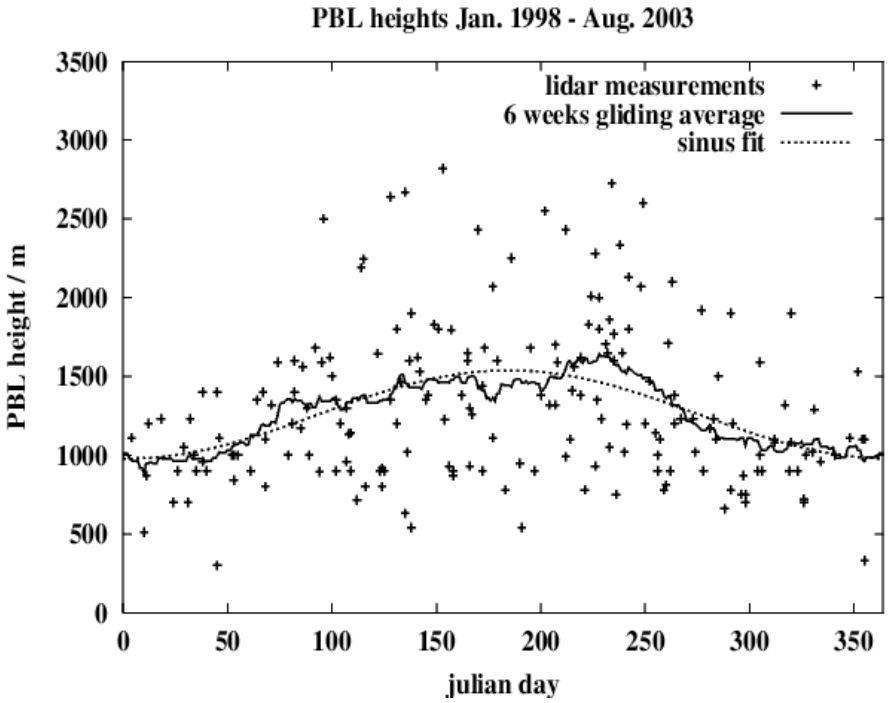


The range of optical depth values observed at Hamburg in the lowest 2 km covers values between 0.06 and 0.9 at 355 nm (Matthias et al., 2004b). Compared to the sunphotometer data at 340 nm (see Table 1), very large values ($\tau_a(340) > 1$) were not found. This difference can be caused by two reasons: the lidar is not covering the whole atmosphere while the sunphotometer does; on the other hand the sunphotometer might be biased to too high values caused by undetected homogeneous cirrus clouds.

With the lidar also the PBL development in the course of the day can be observed. This gives some insight how well the PBL is developed at the ENVISAT overpass time at about 10:30 UT. Assuming a cloud free day, the PBL develops in the morning and reaches its maximum extension around 13-14UT. Earlier in the morning the aerosol is confined in a smaller layer which has only about 50 – 80 % of its maximum thickness in the afternoon. This cannot directly be transferred into differences in the optical depth, because the aerosol extinction values are usually higher in the morning hours which partly compensates the effect of the not yet fully developed boundary layer. As shown previously in this paper the daily average of the aerosol optical depth does not differ much from the average values around 10:30 UT at Helgoland site. Nevertheless, when the vertical extension of the aerosol layer is taken into account in the aerosol models used for the MERIS atmospheric correction, it should be considered that the PBL has not yet fully developed at the overpass time.

## 5. Air mass analysis

To get further insight in the reasons for the large variability of the aerosol properties observed at Helgoland and to see whether other meteorological parameters can be used to get information on the likely aerosol properties, an air mass analysis was carried out for the days when measurements were performed at Helgoland Island.

In total 163 measurement days between April and September of years 2000-2003 are considered. In Table 5 the geographical origin of each air mass following a classification

proposed by Geb (1971) and Vogt (2000) is shown together with the mean values of $\tau_a$, $\alpha$, PW and their standard deviation.

Table 5. Mean characteristics (aerosol optical depth at 500nm $\tau_a(500)$, Ångstrom wavelength exponent $\alpha_{440\text{-}870}$, water vapour content PW of different air masses reaching Helgoland Island, 163 days, 2000-2003.

| Air mass classes (after their geographical origin)* | Code | N | $\tau_a(500)$ | σ | $\alpha_{440\text{-}870}$ | σ | PW (cm) | σ |
|---|---|---|---|---|---|---|---|---|
| **Arctic 6%** | | **10** | **0.13** | **0.04** | **0.76** | **0.36** | **1.68** | **0.50** |
| Maritime (North Sea) | mA | 8 | 0.12 | 0.04 | 0.62 | 0.21 | 1.81 | 0.47 |
| Modified (North Europe) | xA | 2 | 0.16 | 0.03 | 1.34 | 0.12 | 1.17 | 0.23 |
| **Subpolar 31%** | | **51** | **0.16** | **0.10** | **1.09** | **0.39** | **2.06** | **0.53** |
| Maritime (North Atlantic) | mP | 38 | 0.15 | 0.08 | 0.95 | 0.33 | 2.03 | 0.45 |
| Cont. + modified (Russia, N. Europe) | cP+xP | 13 | 0.19 | 0.16 | 1.49 | 0.25 | 2.14 | 0.72 |
| **Warmed subpolar 23%** | | **39** | **0.24** | **0.14** | **1.59** | **0.37** | **2.23** | **0.67** |
| Maritime (warmed over subtropical Sea | mPs | 17 | 0.28 | 0.17 | 1.53 | 0.39 | 2.52 | 0.59 |
| Cont.+modified (warmed over Europe) | cPs+xPs | 22 | 0.20 | 0.09 | 1.65 | 0.36 | 2.01 | 0.65 |
| **Middle latitude 23%** | | **39** | **0.27** | **0.12** | **1.56** | **0.33** | **2.44** | **0.71** |
| Maritime (North Atlantic) | mSp | 5 | 0.27 | 0.06 | 1.29 | 0.28 | 2.56 | 1.03 |
| Cont. + modified (E and W Europe) | cSp+xSp | 34 | 0.27 | 0.13 | 1.60 | 0.32 | 2.42 | 0.67 |
| **Subtropical 14.7%** | | **24** | **0.30** | **0.18** | **1.54** | **0.28** | **2.73** | **0.77** |
| Maritime (Atlantic Subtropics) | mS | 4 | 0.18 | 0.16 | 1.36 | 0.38 | 2.79 | 1.02 |
| Continental + modified (SE Europe) | cS+xS | 20 | 0.32 | 0.18 | 1.57 | 0.26 | 2.72 | 0.75 |

*Air mass classification for Central Europe after Vogt (2000) and Geb (1971). Each air mass is defined by a code (*mA,xA*,....), where *m* is the maritime character, *c* is the continental character and *x* is the modified character, N is the number of the measurement days related to a certain air mass type, $\tau_a(500)$, $\alpha_{440\text{-}870}$ and PW mean values and σ, standard deviation.

Table 6. Mean characteristics (aerosol optical depth at 500nm, Ångström wavelength exponent and water vapour content) and median for four air mass source origins.

| Air mass classes | Code | N | $\tau_a(500)$ | σ | med. | $\alpha_{440\text{-}870}$ | σ | med | PW cm | σ |
|---|---|---|---|---|---|---|---|---|---|---|
| Arctic (mA, xA) | A | 10 | 0.12 | 0.04 | 0.13 | 0.76 | 0.36 | 0.68 | 1.68 | 0.50 |
| North Atlantic (mP, mSp) | NA | 43 | 0.16 | 0.08 | 0.12 | 0.99 | 0.34 | 0.99 | 2.09 | 0.56 |
| Cont Europe (cP,cSp,cPs) | CE | 69 | 0.23 | 0.12 | 0.21 | 1.59 | 0.32 | 1.63 | 2.24 | 0.69 |
| Subtropical (mS, cS, mPs) | S | 41 | 0.29 | 0.17 | 0.21 | 1.53 | 0.33 | 1.63 | 2.64 | 0.70 |

Five classes (arctic, subpolar, warmed subpolar, middle latitude, and subtropical) with two subclasses each (usually maritime and continental) are defined. Due to the low number of values in some of the subclasses, we used mean values instead of the otherwise more appropriate medians to compare among the classes. As expected, differences in the optical depth, the Ångström wavelength exponent and the water vapour content in the different classes can be seen. Arctic and subpolar air masses show lowest values in all parameters, while the subtropical air mass shows the largest values in $\tau_a$ and PW and $\alpha$ values, which are as high as the warmed subpolar and middle latitude classes. If one looks more in detail into the subclasses, the difference between the continental and maritime air masses becomes apparent. Maritime air masses show a lower Ångstrom wavelength exponent and also a lower standard deviation of the optical depth than the continental air masses do. Obviously, the maritime aerosol is much better defined in terms of optical properties than the continental aerosol is.

Therefore, another classification based on the geographic origin of the synoptic air masses seems to be more appropriate. Four new classes are defined: Arctic (A), North Atlantic with maritime character (NA), Continental Europe with continental character (CE)

and Subtropical with both maritime and continental characters (S). These new classes were composed out of the subclasses already given in Table 5. The mean values and the standard deviation as well as the median of the aerosol optical properties ($\tau_a(500)$, $\alpha_{440\text{-}870}$) and the water vapour content PW related to these air mass classes are reported in the Table 6 and Fig.9.

The *Arctic* air mass (A), representing only 6% from all the measurement days, is characterised by the lowest values for $\tau_a(500)$=0.12 ($\sigma_{re}$ =35%) and $\alpha_{440-870}$=0.76 ($\sigma_{re}$ =47%). The *North Atlantic* (NA) air mass with a maritime character occurs more frequently (26% of all cases) and is related to a higher variability of $\tau_a(500)$, $\sigma_{re}$ =51%, but less variability of $\alpha_{440\text{-}870}$, with a mean value of 0.99 and a $\sigma_{re}$ =34%. The lower variability of the $\alpha_{440\text{-}870}$ value is the consequence of the dominance of the maritime aerosols within this air mass. The class *Continental Europe* (CE) is the most frequent of the air masses arriving over this area. It is characterised by a high variability for $\tau_a(500)$, $\sigma_{re}$ =54%, but again the $\alpha_{440\text{-}870}$=1.59 varies only within 20%. This demonstrates the predominance of one aerosol type, the urban one. The *Subtropical* (S) class has a high variability of the aerosol loading (61%) but it is relatively homogeneous in its composition, $\alpha_{440\text{-}870}$ variability is 21%.

Figure 9. Variability of the $\tau_a(500)$ within the origin of the synoptic air mass: A - Arctic, NA - North Atlantic, CE – Continental Europe, S - Subtropical. The inner error bars are the standard deviation of the average (standard error) and the outer bars are the standard deviation of the individual

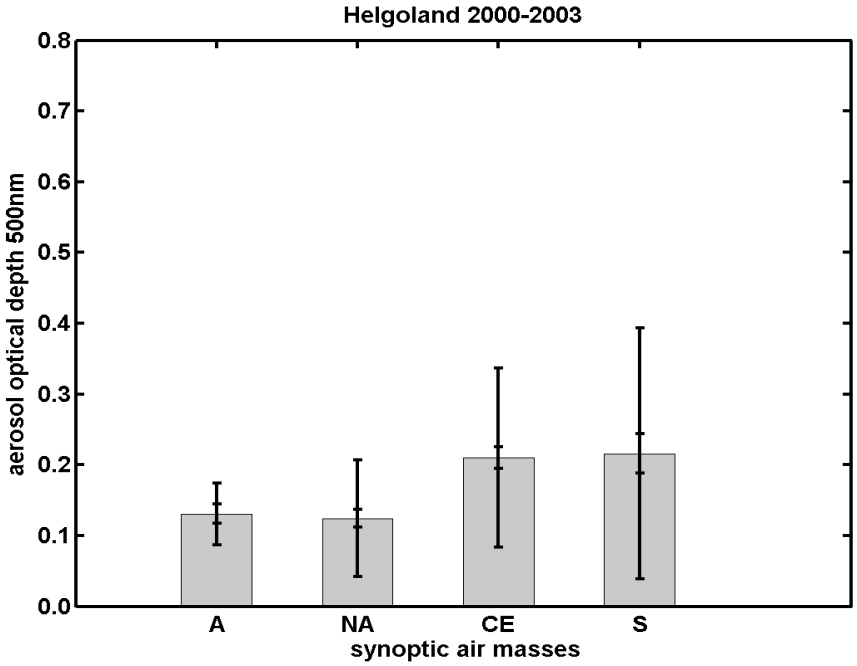


The variability of the aerosol optical depth within these new classes is only weakly reduced compared to the synoptic air mass classes in Table 5 and remains between 35% (A) and 61% (S). Also the Ångstrom wavelength exponent is not better defined (in terms of lower relative variability) in the new classes compared to the first classification. This can be explained by the various aerosol modifications within their lifetime of typically some days in the central European boundary layer. Internal and external mixing, modification by acting as cloud nuclei, removal of soluble parts through precipitation etc. are manifold processes that influence the aerosol optical properties measured at a given time and place in the vicinity of

the North Sea. The air mass in which the aerosols are embedded plays an important role for their optical properties but it cannot tell "the whole story" of all modifications the aerosol particles have undergone. Additionally, local sources like industrial areas at the North Sea coastline, ship traffic and car traffic play an important role for the aerosol loading at Helgoland. Most of these sources are not included in the air mass classification. A previous back trajectories air mass analysis related to lidar aerosol extinction profiles in Hamburg (Matthias and Bösenberg, 2002) demonstrated that air mass derived from local sources show highest values of about $\tau_a(351)=0.32$. Similar to us, Matthias and Bösenberg also reported only a minor decrease in the variability of the aerosol optical depth when a classification related to the air mass origin was established.

The presented air mass analysis demonstrates that aerosol optical properties, as aerosol optical depth, Ångström wavelength exponent and the related water vapour, which are important parameters for the atmospheric correction algorithm of MERIS data, can only be predicted with high errors from the surface synoptic charts for the coastal regions of the North Sea. The method produced good results in other regions as the low populated parts of Canada (Smirnov et al., 1994; 1996) and over the oceans (Smirnov et al., 1995), but it is less appropriate for the highly industrialised regions in northern and central Europe, characterised by a high level of anthropogenic local sources.

## 6. Consequences for the atmospheric correction of coastal ocean color data

The dominant signal in ocean colour remote sensing using earth observation satellites comes from the atmosphere. The path radiance, i.e. the radiance reflected by the atmosphere along the path of observation, can surmount the water leaving radiance by a factor in the order of ten. Thus, this path radiance has to be determined and subtracted very accurately. Furthermore, also the transmittance of the water leaving radiance through the atmosphere has to be calculated. Both calculations form the atmospheric correction, which is the most critical step in ocean colour remote sensing.

The standard procedure is to determine the path radiance at a number of bands in the red and near infrared spectral range, where the scattering by water and its constituents does not contribute to this signal due to the high absorption of pure water. The path radiances and transmittances at these bands are then extrapolated across the visible spectrum, for which the atmospheric correction has to be performed. This procedure requires a reliable model of the spectral scattering properties of aerosols. Any small error in the extrapolation causes a large error in the determination of the water leaving radiance and thus in the determination of e.g. phytoplankton concentration.

In the case of the atmospheric correction procedure for coastal waters of the North Sea an insufficient correction in particular in the blue part of the spectrum was realised so that the calculated path radiance derived from top of atmosphere reflectances was higher than the radiance reflectance measured from a ship. An analysis of the Ångström wavelength exponents of the aerosol model revealed a maximum Ångström wavelength exponent of $\alpha = 1.2$, which was far below the median of all points (see Table 2) recorded of the sunphotometer at Helgoland of $\alpha = 1.6$. A careful analysis showed that the size distribution of some aerosol components was not adequately represented for a coastal site. After a modification of the size distribution, in particular of the small components (water soluble, urban aerosol), and a recalculation, an aerosol optical depth could be achieved as measured with the sunphotometer.

Figure 10. Aerosol optical depth for a maritime atmosphere with the sets of the size distributions. The first 2 km of the model atmosphere are characterized by maritime aerosols with $\tau_a = 0.2$ at $\lambda = 550$ nm and Ångström wavelength exponent old = 0.3835, new = 0.8140. Please note the different ordinate scales in Fig. 10 and Fig. 11.

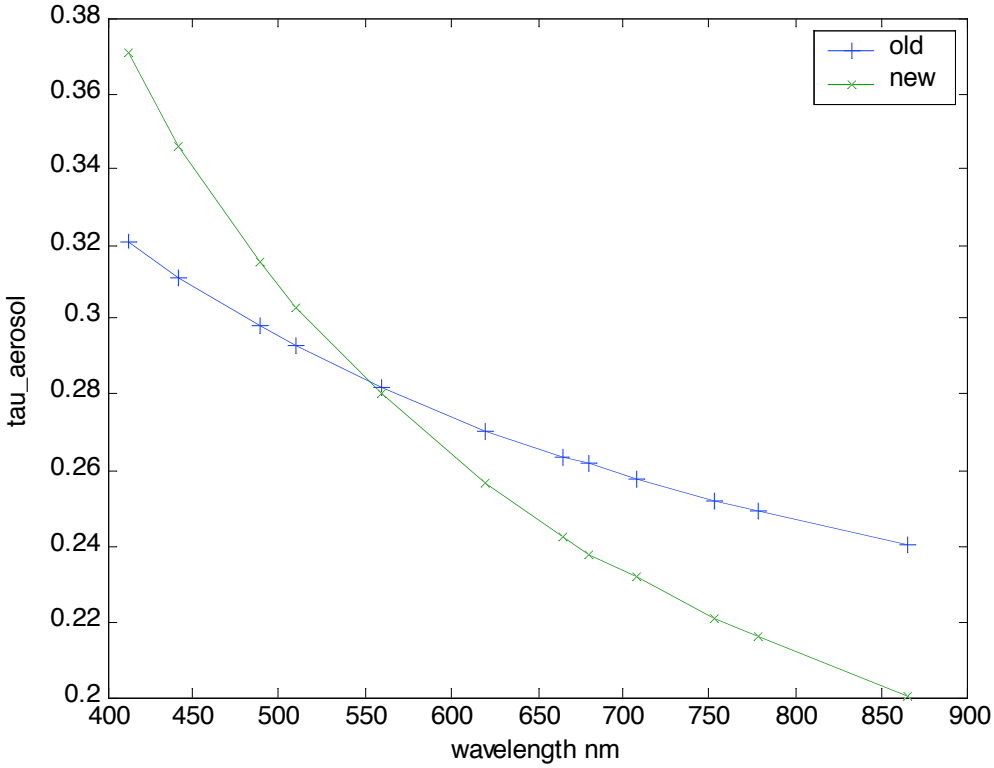


The modified aerosol model now allows to meet the frequency distribution of the Ångström wavelength exponent of Helgoland (and many other coastal sites).

Fig. 10 shows the aerosol total optical depth of a maritime atmosphere before and after correction and Fig. 11 the same for an urban atmosphere. The two different sets of aerosol models that were applied are summarised in Table 7.

The resulting path radiance reflectance for the urban atmosphere (Fig. 12) shows a significant increase in the blue part of the spectrum, which is in the order of the water leaving radiance reflectance of coastal waters as present in the German Bight.

Figure 11. As Fig. 10 but for an urban atmosphere. The first 2 km of the model atmosphere are characterized by urban aerosols with $\tau_a = 0.5$ at $\lambda = 550$ nm and an Ångström wavelength exponent of old = 1.14 and new= 1.61. Please note the different ordinate scales in Fig. 10 and Fig. 11.

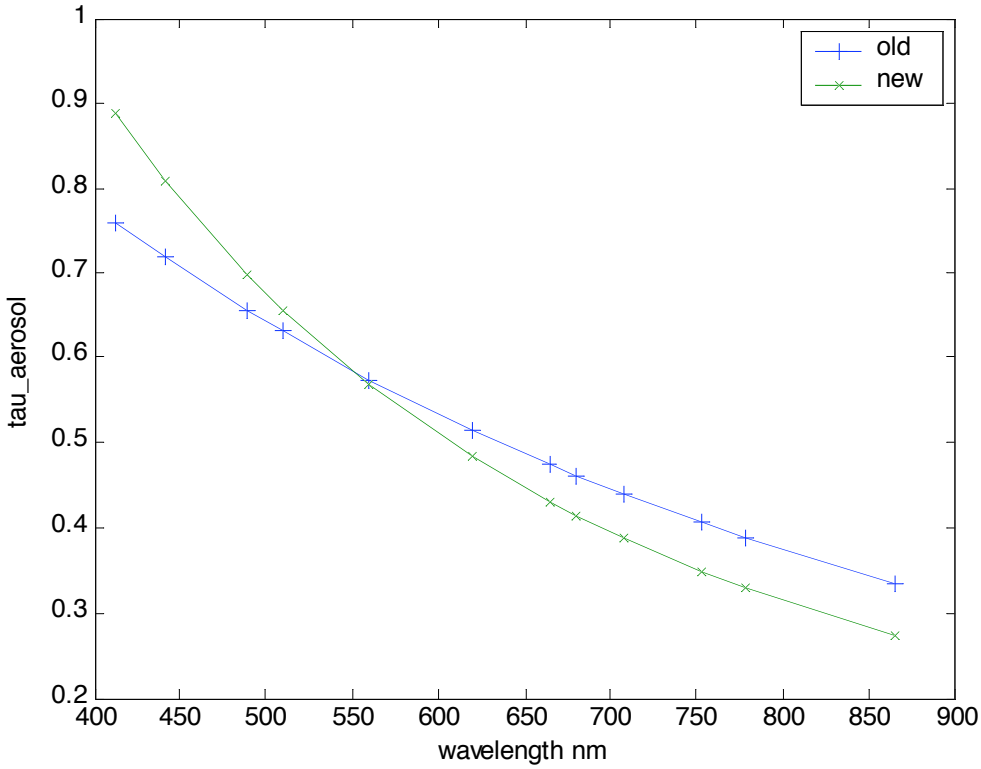


Table 7. Aerosol optical depths at $\lambda$=550nm and total ozone values for the maritime and urban atmosphere (composed of maritime, urban, continental and stratospheric aerosols) used for simulating the radiative transfer using a Monte Carlo photon tracing model, all calculations are for wind speed 3 m/s, sun 45 deg.

| Atmosphere type | Maritime | Urban | Continental | Stratospheric | ozone DU |
|---|---|---|---|---|---|
| **Maritime** | 0.2 | 0.0 | 0.0825 | 0.0015 | 289 |
| **Urban** | 0.0 | 0.5 | 0.0825 | 0.0015 | 289 |

Figure 12. Nadir path radiance at the top of atmosphere for the urban atmosphere.

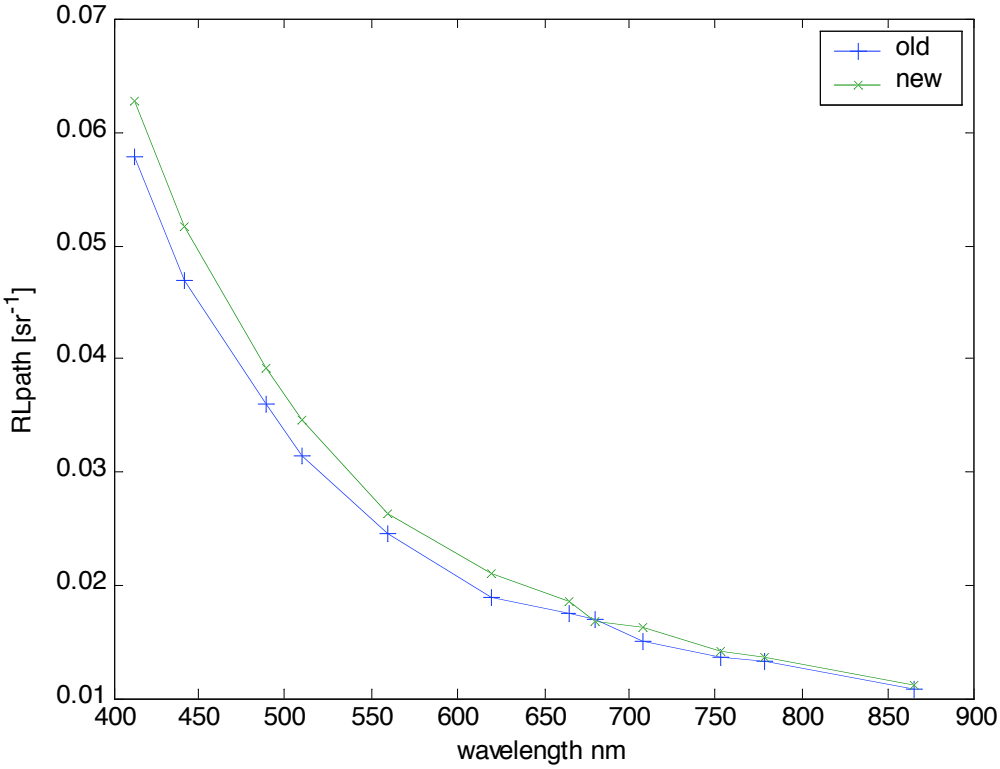


## 7. Conclusions

Similarities in the aerosol optical properties derived from AERONET data are found between the Helgoland island, the coastal site Ooostende and the urban sites of Hamburg and Lille. A regional aerosol climatology over the southern North Sea region has to take into account the data from all these four sites. It could be shown that the aerosol optical properties at Helgoland differ significantly from those at other maritime sites (e.g. Azores Island) or clean sites at the west coast of Europe (e.g. Rame Head, United Kingdom)

The range of values for the aerosol optical depth at 500nm within each site and its seasonal variation is similar at all selected AERONET sites. Links between the aerosol optical properties and the synoptic air masses are found for Helgoland, however the errors in the a priori prediction is about 34%-61% for $\tau_a(500)$ and 20-47% for $\alpha_{440-870}$. High similarities in the lognormal distribution of the aerosol optical depth daily average at 340 and 500 nm and the frequency distribution of the Ångström wavelength exponent $\alpha_{440-870}$ are found among the sites at Hamburg, Oostende and Lille. They are classified as urban sites with some maritime influence. Helgoland shows some differences, a larger influence of maritime aerosols can be observed, but the site is still closer to Hamburg, Lille and Oostende as it is to Rame Head or the Azores.

The average value of the single scattering albedo $\omega_0(550)$~0.95 for Helgoland also describes a "polluted-maritime" site, with slightly less absorbing aerosols than those found at Hamburg, Oostende and Lille. However, the differences remain within the uncertainty limits.. The averaged value of the real part of the refractive index is the same for Helgoland and Oostende, n(550)=1.42 and it is spectrally independent. This value is higher than that reported for the maritime sites, n(550)=1.37 for Lanai, Bermuda and Kaashidhoo (Smirnov et al., 2003). The single scattering albedo and the refractive index found at Hamburg and Lille ($\omega_0(550)$= 0.94/0.93, n = 1.40/1.39) are similar to that reported for other urban sites (Dubovik et al., 2002).

The volume particle size parameters derived at Helgoland show equal values of the particle volume concentration in the fine and the coarse mode. This is different at the other sites where the fine mode dominates and shows again the larger influence of maritime aerosols at Helgoland. However, they do not dominate the aerosol optical properties. The vertical distribution of the aerosol can be determined by regular lidar measurements. It was shown that the optical depth values from the Raman lidar at Hamburg are in good agreement with the sunphotometer measurements.

The MERIS atmospheric correction of imagery captured over coastal turbid waters can be improved if the range of aerosol optical properties determined by the actual climatology (see Table 1) would be considered. Generally, this aerosol climatology could be used also for others ocean colour sensors for the atmospheric correction over this region. The limits of this climatology are resulting from the relatively short time series available at each site, which can not take into account all possible atmospheric conditions with different aerosol loadings. This database is not only related to the coastal continental region but also to the conditions 70 km away from the coast as represented by the measurements on Helgoland island. However, it cannot deliver a complete picture about the variation of the aerosol optical properties over the whole North Sea coastline, where the atmospheric correction is also of high importance.

The conclusion for atmospheric correction of coastal water remote sensing data is that in particular the Ångström wavelength exponents of the aerosol model used for atmospheric correction should be compared with measured data of the site under consideration, and that the Ångström wavelength exponents of a typical maritime atmosphere are not sufficient for most coastal sites. Since many sunphotometer measurements confirm that an Ångström wavelength exponent around $\alpha$ =1.6 can be regarded as a median value for coastal sites, the aerosol model for atmospheric correction of coastal remote sensing data should include Ångström wavelength exponents at least up to a value of $\alpha = 2$.

**Acknowledgements.**

We thank the (PI investigators) and their staff for establishing and maintaining the sites used in this investigation: Hamburg – Jens Bösenberg, Max-Planck Institut für Meteorologie; Oostende – Kevin Ruddick and Jean-Pierre De Blauwe, MUMM; Lille – Didier Tanré, Laboratoire d'optique atmosphérique; Rame Head –Tim Smyth and Samantha Lavender, Plymouth Marine Laboratory; Azores – Charles McClain and Christophe Pietras, NASA GSFC, SIMBIOS Project. Thanks to Peter Kipp, Institute for Coastal research, GKSS and Firma Jebo for establishing and maintaining the Helgoland AERONET site. We also thank the AERONET staff for the data collection, processing and calibration. We thank Prof. Wehry, Institut für Meteorologie der Freien Universität Berlin for the meteorological data. The financial support of this work by the European Commission under the grants EVR1-CT-1999-40003 (EARLINET) and EVG1-CT-2000-00034 (NAOC) is gratefully acknowledged.

## Glossary

| | |
|---|---|
| $\tau_a(500)$, $\tau_a(340)$ | Aerosol optical depth at 500nm and 340nm |
| $\alpha_{440-870}$ | Ångström wavelength exponent between 440 and 870 nm |
| $n(\lambda) + ik(\lambda)$ | Refractive index, real and imaginary part |
| $\omega_0(550)$ | Single scattering albedo at 550nm |
| $r_{Vi}$, $\sigma_i$ | Median radius of mode i (total, coarse, fine) and width of the particle size distribution of mode i (total, coarse, fine) |
| $C_{vi}$ | Particle volume concentration of mode i (total, coarse, fine) |

| | |
|---|---|
| PW | Water vapour content (cm) |
| m, s | Mean and standard deviation of the lognormal distribution |
| $\sigma$ | Standard deviation of the individual value |
| $\gamma$ | Skewness |
| $\sigma_{re}$ | Relative standard deviation |
| $\sigma_m$ | Standard error or the standard deviation of the average |

**Notation**

| | |
|---|---|
| AERONET | Aerosol Robotic Network |
| EARLINET | European Aerosol Research Lidar Network |
| GADS | Global Aerosol Data Set |
| MERIS | Medium Resolution Imaging Spectrometer |
| NN | Neural network |
| OPAC | Optical properties of aerosols and clouds |
| PBL | Planetary boundary layer |
| TOA | Top of the atmosphere |
| WCP | World Climate Research Programme |

**References**


Antoine, D., Morel, A., 1999. A multiple scattering algorithm for atmospheric correction of remotely sensed ocean colour (MERIS instrument): principle and implementation for atmospheric carrying various aerosols including absorbing ones. Int. J. Rem. Sens. 29/5, 1875-1916.

Antoine, D., Morel, A., 2000. MERIS ATBD 2.7. Atmospheric correction over the ocean (Case 1 waters), ESA Publication.

Ansmann, A., Wandinger, U., Riebesell, M., Weitkamp, C., Michaelis, W., 1992. Independent measurement of extinction and backscatter profiles in cirrus clouds by using a combined Raman elastic-backscatter lidar. Appl. Opt. 31, 7113-7131.

Ansmann, A., Wagner, F., Althausen, D., Müller, D., Herber, A., Wandinger, U., 2001. European pollution outbreaks during ACE 2: Lofted aerosol plumes observed with Raman lidar at the Portuguese coast. J. Geophys. Res. 106, 20725-20733.

Behnert, I., Matthias, V., Doerffer, R., 2004. Aerosol optical thickness and its spectral dependence derived from sunphotometer measurements over the southern North Sea coastal region. Proceedings of the AERONET/PHOTONS Workshop, May 2004 El Arenosillo.

Bohren, C.F., Huffman, D.R. 1983. Absorption and Scattering of Light by Small Particles. Wiley & Sons, Inc., New York, US. 550 pp.

Bösenberg, J., Alpers, M., Althausen, D., Ansmann, A., Böckmann, C., Eixmann, R., Franke, A., Freudenthaler, V., Giehl, H., Jäger, H., Kreipl, S., Linne, H., Matthias, V., Mattis, I., Müller, D., Sarközi, J.,. Schneidenbach, L, Schneider, J., Trickl, T., Vorobieva, E., Wandinger U., Wiegner, M., 2001. The German Aerosol Lidar Network: Methodology, Data, Analysis. MPI report 317, Max-Planck-Institut für Meteorologie, Hamburg.

Bösenberg, J., Matthias, V., Amodeo, A., Amiridis, V., Ansmann, A., Baldasano, J. M., Balin, I., Balis, D., Böckmann, C., Boselli, A. , Carlsson, G., Chaikovsky, A., Chourdakis, G., Comeron, A., De Tomasi, F., Eixmann, R., Freudenthaler, V., Giehl, H., Grigorov, I., Hagard, A., Iarlori, M., Kirsche, A., Kolarov, G., Komguem, L., Kreipl, S., Kumpf, W., Larcheveque, G., Linne, H., Matthey, R., Mattis, I., Mekler, A., Mironova, I., Mitev,

V., Mona, L., Müller, D., Music, S., Nickovic, S., Pandolfi, M., Papayannis, A., Pappalardo, G., Pelon, J., Perez, C., Perrone, R. M., Persson, R., Resendes, D. P., Rizi, V., Rocadenbosch, F., Rodrigues, J. A., Sauvage, L., Schneidenbach, L., Schumacher, R., Shcherbakov, V., Simeonov, V., Sobolewski, P., Spinelli, N., Stachlewska, I., Stoyanov, D., Trickl, T., Tsaknakis, G., Vaughan, G., Wandinger, U., Wang, X., Wiegner, M., Zavrtanik M., Zerefos, C., 2003. A European Aerosol Research Lidar Network to Establish an Aerosol Climatology. MPI report 348, Max-Planck-Institut für Meteorologie, Hamburg.

Carlson, T.N., Prospero, J.M., 1972. The large-scale movement of Saharan air outbreaks over the northern equatorial Atlantic. J. Appl. Meteorol. 11, 283-297.

Coulter, R.L., 1979. A comparison of three methods for measuring mixing-layer height. J. Appl. Meteorol., 18, 1495-1499.

Doerffer, R., Schiller, H., 1997. MERIS ATBD 2.12. Pigment index, sediment and "gelbstoff" retrieval from directional water leaving radiance reflectance using inverse modelling technique, ESA Publication.

Doerffer, R., Schiller, H., 2002. A neural network based atmospheric correction procedure for the retrieval of water constituent concentrations in turbid case II water from MERIS data. Proceeding of Ocean Optics XVI, Santa Fe, November 2002.

Dubovik, O., King, M.D., 2000. A flexible inversion algorithm for retrieval of aerosol optical properties from Sun and sky radiance measurements. J. Geophys. Res. 105, 20 673-20 696.

Dubovik, O., Smirnov, A., Holben, B. N., King, M.D., Kaufman, Y.J., Eck, T.F., Slutsker, I., 2000. Accuracy assessments of aerosol optical properties retrieved from AERONET sun and sky-radiance measurements. J. Geophys. Res. 105, 9791-9806.

Dubovik, O., Holben, B.N., Eck, T.F., Smirnov, A., Kaufman, Y.J., King, M.D., Tanre, D., Slutsker, I., 2002. Variability of absorption and optical properties of key aerosol types observed in worldwide locations. J. Atmos. Sci. 59, 590-608.

Eck, T.F., Holben, B.N., Reid, J.S., Dubovik, O., Smirnov, A., O'Neill, N.T., Slutsker, I., Kinne, S., 1999. Wavelength dependence of the optical depth of biomass burning, urban and desert dust aerosols. J.Geophys. Res. 104. 31 333-31 350.

Geb, M., 1971. New aspects and interpretations of air masses and fronts concepts (in German: Neue Aspekte und Interpretationen zum Luftmassen- und Frontenkonzepten), printed by Institut für Meteorologie der Freien Universität Berlin, Meteorologischen Abhandlungen Vol. 109/2.

Gordon, H.R., 1997. Atmospheric correction of ocean color imagery in the Earth Observing System era. J.Geopys. Res. 102D, 17081-17106.

Halthore, R.N., Eck, T.F., Holben, B.N., Markham, B.L., 1997. Sunphotometric measurements of atmospheric water vapour column abundance in the 940-nm band. J. Geophys. Res. 102, 4343-4352.

Hess, M., Koepke, P., Schult, I., 1998. Optical properties of aerosols and clouds: the software package OPAC. Bulletin of the American Meteorology 79/5, 831-844.

Holben B.N., Eck, T.F., Slutsker, I., Tanre, D., Buis, J.P., Setzer, A., Vermote, E., Reagan, J.A., Kaufman, Y., Nakajima, T., Lavenu, F., Jankowiak, I., Smirnov, A., 1998. AERONET - A federated instrument network and data archive for aerosol characterization. Rem. Sens. Environ. 66, 1-16.

Holben, B.N., Tanre, D., Smirnov, A., Eck, T.F., Slutsker, I., Abuhassan, N., Newcomb, W., Schafer, J., Chatenet, B., Lavenue, F., Kaufman, Y.J., Vande Castle, J., Setzer, A., Markham, B., Clark, D., Frouin, R., Halthore, R., Karnieli, A., O'Neill, N.T., Pietras, C., Pinker, R.T., Voss, K., Zibordi, G., 2001. An emerging ground-based aerosol climatology: Aerosol Optical Depth from AERONET. J. Geophys. Res. 106, 12 067-12 097.

Hoyningen-Huene, W.v. and Raabe, A., 1987. Maritime and continental air mass differences in optical aerosol extinction data. Beitr. Phys. Atmosph., 60(1), 81-88.

Junge, C., 1952. Gesetzmäβigkeiten in der Größenverteilung atmosphärischer Aerosole über dem Kontinent. 35, p.261-277, Deutscher Wetterdienst in der US-Zone.

Kaufman, Y.J., Tanré, D., Gordon, H.R., Nakajima, T., Lenoble, J., Frouin, R., Grassl, H., Herman, B.M., King M.D., Teillet, P.M., 1997. Passive remote sensing of tropospheric aerosol and atmospheric correction for the aerosol effect. J. Geophys. Res. 102/D14, 16815-16830.

Kaufman, Y.J., Tanré, D., Dubovik, O., Karnieli A., Remer, L.A., 2001a. Absorption of sunlight by dust as inferred from satellite and ground-based remote sensing. Geoph. Res. Lett. 28, 8, 1479-1482.

Kaufman, Y.J., Smirnov, A., Holben, B.N., Dubovik, O., 2001b. Baseline maritime aerosol: methodology to derive the optical depth and scattering properties. Geoph. Res. Lett. 28, 3251-3254.

Koepke, P., Hess, M., Schult, I., Shettle, E.P., 1997. Global Aerosol Data Set. Report No.243, Max-Planck-Institute for Meteorology, Hamburg.

Matthias, V., Bösenberg, J., 2002. Aerosol climatology for the planetary boundary layer derived from regular lidar measurements. ATMOS.RES. 63, 221-245.

Matthias, V., Freudenthaler, V., Amodeo, A., Balin, I., Balis, D., Chaykovski, A., Chourdakis, G., Comeron, A., Delaval, A., de Tomasi, F., Eixmann, R., Hagard, A., Komguem, L., Kreipl, S., Matthey, R., Mattis, I., Rizi, V., Rodrigues J., Wang, X., 2004a. Aerosol lidar intercomparison in the framework of the EARLINET project. 1. Instruments, Appl. Opt. 43, 961-976.

Matthias, V., Balis, D., Bösenberg, J., Eixmann, R., Iarlori, M., Komguem, L., Mattis, I., Papayannis, A., Pappalardo, G., Perrone, M.R., Wang, X., 2004b. Vertical aerosol distribution over Europe: Statistical analysis of Raman lidar data from 10 European Aerosol Research Lidar Network (EARLINET) stations. J.Geophys. Res. 109, D18201, doi: 10.1029/2004JD004638.

Menut, L., Flamant, C., Pelon J., Flamant, P., 1999. Urban boundary layer height determination from lidar measurements over the Paris area. Appl. Opt. 38, 945-954.

Mie, G., 1908. Beitrage zur Optik trüber Medien speziell kolloidaler Metallösung. Ann. Phys. 25, 377-445.

Minikin A., Petzold, A. , Strom, J., Krejci, R., Seifert, M., van Velthoven, P., Schlager, H., Schumann, U., 2003. Aircraft observation of the upper tropospheric fine particle aerosol in the Northern and Southern Hemispheres at midlatitudes. Geoph. Res. Lett. 30, 10, 1503, doi:10.1029/2002GL016458.

O'Neill, N.T., Ignatov, A., Holben, B.N., Eck, T.F., 2000. The lognormal distribution as a reference for reporting aerosol optical depth statistics; Empirical tests using multi-year, multi-site AERONET sunphotometer data. Geophys. Res. Lett. 27, 20, 3333-3336,

Papayannis, A., Amiridis, A., Baldasano, J., Balin, I., Balis, D., Boselli, A., Chaikovsky, A., Chatenet, B., Chourdakis, G., Freudenthaler, V., Frioud, M., Herman, J., Iarlori, M., Kreipl, S., Larcheveque, G., Matthey, R., Mattis, I., Müller, D., Pandolfi, M., Pappalardo, G., Pelon, J., Perrone, M.R., Rizi, V., Rodriquez, A., Sauvage, L., Sobolewski, P., Spinelli, N., de Tomasi, F., Trickl, T., Wiegner, M., 2004. Continental-scale vertical profile measurements of free tropospheric Saharan dust particles performed by a coordinated ground-based European Aerosol Research Lidar Network (EARLINET Project): A two-cases study from the first year of observations. Atmos. Chem. Phys. (submitted).

Park, Y., De Cauwer, V., Nechaud, B., Ruddick, K., 2003. Validation of MERIS water products for Belgian coastal waters: 2002-2003. Proceedings of the MERIS and

AATSR Calibration and Geographical validation workshop, Frascati October 2003, ESA Publication.

Remer, L.A., Kaufman, Y.J., 1998. Dynamic aerosol model: Urban/industrial aerosol. J. Geophys. Res. 103, 13859-13871.

Robles Gonzalez, C., Schaap, M., de Leeuw, G., Builjes, P.J.H., van Loon, M., 2003. Spatial variability of aerosol properties over Europe derived from satellite observations and comparison with model calculations. Atmos. Chem. Phys. 3, 521-533.

Rollin, E.M., 2000. An introduction to the use of Sun-photometry for the atmospheric correction of airborne sensor data. Activities of the NERC EPFS in support of the NERC ARSF. ARSF Annual Meeting, Keyworth, Nottingham, UK, 22pp.

Russell, P.B., Uthe, E.E., Ludwig, F.L., Shaw, N.A., 1974. A comparison of atmospheric structure as observed with monostatic acoustic sounder and lidar techniques. J. Geophys. Res. 79, 5555-5566.

Shettle, E.P., Fenn, R.W., 1979. Models of aerosols of lower troposphere and the effect of humidity variations on their optical properties. AFCRL Techn. Rep. 79 0214, Air Force Cambridge Research Laboratory, Hanscom Air Force Base, MA, 100pp.

Smirnov, A., Royer, A., O'Neill, N.T., Tarussov, A., 1994. A study of the link between air mass type and atmospheric optical parameters. J. Geophys. Res. 99, 20 967-20 982.

Smirnov, A., Villevalde, Yu., O'Neill, N.T., Royer, A., Tarussov, A., 1995. Aerosol optical depth over the oceans: analysis in terms of synoptic air mass types. J. Geophys. Res. 100, 16 639-16 650.

Smirnov, A., O'Neill, N.T., Royer, A., Tarussov, A., McArthur, B., 1996. Aerosol optical depth over Canada and the link with synoptic air mass types. J. Geophys. Res. 101, 19 299-19 318.

Smirnov, A., Holben, B.N., Eck, T.F., Dubovik, O., Slutsker, I., 2000. Cloud screening and quality control algorithms for the AERONET database. Rem. Sens. Env. 73, 337-349.

Smirnov, A., Holben, B.N., Kaufman, Y.J., Dubovik, O., Eck, T.F., Slutsker, I., Pietras, C., Halthore, R., 2002a. Optical Properties of Atmospheric Aerosol in Maritime Environments. J. Atmos. Sci. 59, 501-523.

Smirnov, A., Holben, B.N., Eck, T.F., Slutsker, I., Chatenet, B., Pinker, R.T. 2002b. Diurnal variability of aerosol optical depth observed at AERONET (Aerosol Robotic Network) sites. Geophys. Res. Lett. 29 (23), 2115, doi:10.1029/2002GL016305.

Smirnov, A., Holben, B.N., Dubovik, O., Frouin, R., Eck, T.F., Slutsker, I., 2003. Maritime component in aerosol optical models derived from Aerosol Robotic Network data, J. Geophys. Res. 108(D1), 4033, doi:10.1029/2002JD002701.

Tanre, D., Kaufman, Y.J., Holben, B.N., Chatenet, B., Karnieli, A., Lavenu, F., Blarel, L., Dubovik, O., Remer, L.A., Smirnov, A., 2001. Climatology of dust aerosol size distribution and optical properties derived from remotely sensed data in the solar spectrum. J. Geophys. Res. 106, 18 205-18 218.

Vogt, H., 2000. Erklärungen zur Berliner Wetterkarte (Explications to the weather chart of Berlin), in Beitrage des Instituts für Meteorologie der Freien Universität Berlin.

WCP - 112, 1986. World Climate Research Program - A preliminary cloudless standard atmosphere for radiation computation. Int. Ass. for Meteor. and Atm. Phys., Radiation Commission, WMO/TD-NO. 24, 53pp.

Wiscombe, W.J, 1996. Mie Scattering Calculations: Advances in Technique and Fast, Vector-Speed Computer Codes. NCAR/TN-140+STR, NCAR Technical Note, Atmospheric Analysis and Prediction Division, National Center for Atmospheric Research, Boulder, Colorado, 64pp.